

Harmonic Solid Theory of Photoluminescence in the High Field Two-Dimensional Wigner Crystal

S. Kadiyalam[†], H.A. Fertig[‡] and S. Das Sarma[†]

[†]*Department of Physics, University of Maryland, College Park, Maryland 20742-4111*

[‡]*Department of Physics and Astronomy, University of Kentucky, Lexington, Kentucky 40506-0055*

Motivated by recent experiments on radiative recombination of two-dimensional electrons in acceptor doped GaAs-AlGaAs heterojunctions as well as the success of a harmonic solid model in describing tunneling between two-dimensional electron systems, we calculate within the harmonic approximation and the time dependent perturbation theory the line shape of the photoluminescence spectrum corresponding to the recombination of an electron with a hole bound to an acceptor atom. The recombination process is modeled as a sudden perturbation of the Hamiltonian for the in-plane degrees of freedom of the electron. We include in the perturbation, in addition to changes in the equilibrium positions of electrons, changes in the curvatures of the harmonically approximated potential. The computed spectra have line shapes similar to that seen in a recent experiment. The spectral width, however, is roughly a factor of 3 smaller than that seen in experiment if one assumes a perfect Wigner crystal for the initial state state of the system, whereas a simple random disorder model yields a width a factor of 3 too large. We speculate on the possible mechanisms that may lead to better quantitative agreement with experiment.

PACS numbers: 73.20Dx ; 71.45.-d ; 78.20.Ls ; 73.40.Hm

I. INTRODUCTION

The properties of non-relativistic electrons in a jellium background have been a subject of experimental and theoretical interest. In its quantum mechanical description, the Planck's constant \hbar and the electron charge e and mass m , conveniently provide the natural scales for measuring the largeness/smallness of all other input parameters (such as the average density of electrons) that may enter the Hamiltonian of the system. Using the variational principle, Wigner¹ pointed out that at low electron densities a (three dimensional) system of electrons with a wavefunction corresponding to a "solid crystalline state" would have lower energy than that calculated perturbatively beginning with the non-interacting electron "liquid" ground state. Experimental evidence for this crystalline "phase" was later presented for electrons on the (two dimensional) surface of Helium.² Variational calculations by Tanatar and Ceperley³ on a two dimensional electron system (2DES) supported these observations by indicating a phase transition when the electron density n was small: $(\pi n)^{-\frac{1}{2}} = 37 \pm 5$ ($= r_s$ in units of $\frac{\hbar^2}{me^2}$). In recent years, the 2DES has been realized at the interface of semiconductor heterostructures. In these experiments, the application of a perpendicular magnetic field B provides a second parameter, the filling factor ν ($= \frac{2\pi\hbar cn}{|e|B}$), the variation of which has resulted in the experimental observation of a rich phase diagram including integer⁴ and fractional quantum Hall states⁵ at particular values of ν . Using the Lindemann melting criterion, the solid-liquid phase boundary (in the r_s - ν plane) for the 2DES has also been computed.⁶ This calculation shows that the density at which the liquid to solid transition occurs increases monotonically with the magnetic field. It also shows that even in the extreme quantum limit ($r_s \rightarrow 0$)

the solid phase exists below $\nu = 0.2$.

Several recent experiments have reported on the radiative recombination of electrons from the 2DES at the junction of a GaAs-AlGaAs single heterostructure with acceptor atoms a certain distance from the interface in the GaAs layer.⁷⁻¹⁰ For certain low values of ν the photon spectrum in these experiments has been interpreted as corresponding to the recombination of an electron (of the 2DES) in the Wigner solid phase with localized holes bound to the acceptor atoms. Accepting this interpretation we calculate here the line shape of the spectrum from the Wigner solid and compare it with the experimental curve.⁸ Our goal is to explicitly investigate whether the theoretical consequences of this interpretation agree with the actual experimental observations of Ref. 8.

The model we adopt is as follows. We consider an electron solid in which an unoccupied localized state out of the plane of the 2DES is available for an electron to tunnel into. One of the electrons - presumably the one closest to it - is assumed to tunnel into the available state, leaving behind a set of electrons that is no longer in an equilibrium configuration. This configuration may be represented as a distorted solid around some new equilibrium configuration, and these distortions may be written as a linear combination of the phonon states of the Wigner crystal. The squared amplitude for each final state then represents the probability of finding the system in some definite state of the final Hamiltonian; the difference in energy between this state and the initial state is released as a photon. Thus one expects a broad photon spectrum due to the many possible final phonon states.

We consider both the limit of a perfect electron solid for the initial state, and one in which several charged impurities may be located in the acceptor plane. The motivation for the latter model is that the experiments with which we wish to compare - time resolved photolu-

minescence (PL) spectroscopy - measures the spectrum only after a waiting time has passed. This not only allows the electrons to settle down into a quasiequilibrium state, but also allows the acceptors that are closest to positions of the electrons in the 2DES to absorb electrons from it. Thus, after a sufficient waiting perood, the initially neutral acceptor atoms, that are meant to probe the system, become a source of disorder for it. The disorder associated with the acceptor positions, therefore, may affect the PL spectrum.

Because the holes closest to electrons are eliminated quickly, we assume that the holes in our problem are relatively far from any electrons. In the case of a perfect crystalline initial state, we assume that hole to be located near an interstitial position of the lattice.⁷ For a disordered initial state, we search for locations in the plane that are far from any electron and presume these are good candidates for locations of holes that may contribute to PL long after the initial excitation. In either case, we find PL lineshapes that are in good qualitative agreement with experiment.⁸ However, for a perfect Wigner crystal, we find a PL spectral width approximately a factor of 3 narrower than the experimental results, whereas our random disorder model yields a lineshape a factor of 3 broader than experiment. This quantitative disagreement may arise from correlations in the acceptor positions which our random disorder model neglects.

Our approach is unusual in that we allow not just for shifts in the electronic positions, but also for changes in the phonon frequencies after the recombination event has occurred. This can be a potentially important improvement, because the removal of an electron effectively removes a degree of freedom, and may introduce localized phonon states in the vicinity of the (charged) acceptor atom. Previous approaches to sudden switching problems such as this have assumed the phonon spectrum to be the same around the initial and final equilibrium configurations of the electrons.^{11,12}

This paper is organized as follows. In section II we describe our model in details and explain how the PL spectrum may be derived from it. Section III is a discussion of our results, and we conclude with a summary in section IV. Because we employ novel theoretical techniques not readily available in the literature, our appendices are fairly complete, which, however, can be skipped unless one is interested in following the technical details of our calculation. Detail of the calculation are given in these Appendices.

II. THEORETICAL APPROACH

The harmonic solid model has been successfully used previously to study tunneling between two 2DESS in a strong perpendicular magnetic field.¹¹ The quantitative success of this model in explaining the experimental I-V characteristics¹³ has motivated us to adopt a *similar*

model for computing the PL spectrum. We therefore determine the Hamiltonian *for the x-y degrees of freedom* of the 2DES (assumed to be in the x-y plane) within the harmonic approximation. This approach could be considered to be complimentary to the previous Hartree-Fock theory for the phonon shakeup effects on PL.¹⁴

The system studied consists of a *finite* number of electrons in the x-y plane within a boundary of the shape of a parallelogram that is commensurate with a triangular lattice. In the model we study there are *always* some electrons that are pinned - they may be in the x-y plane and/or below the plane corresponding to the charged acceptor atoms. The electron-electron interactions are however not purely Coulomb like - this is primarily due to the application of periodic boundary conditions which simulates an infinite system by repeating the finite system at integral multiples of *its* lattice constants. (These lattice constants, \vec{a}_1 and \vec{a}_2 , correspond to the parallelogram that serves as a unit cell that contains the entire finite system.) In some of the cases studied here the Coulomb interaction has been “softened” to the form $(r^2 + z^2)^{-\frac{1}{2}}$ to account for the finite extent of the 2DES in the z direction.

The process of electron capture from the 2DES by the acceptor atom is modeled to be a sudden perturbation of the Hamiltonian corresponding to the x-y degrees of freedom of the 2DES. The recombination process is represented through the introduction of a fictitious parabolic external potential in the final Hamiltonian that confines the x-y coordinates of one of the electrons to a position \vec{r}_0 corresponding to the x-y coordinates of the acceptor atom that is capturing the electron. The change in the z coordinate of this recombining electron is also reflected as a sudden perturbation of the corresponding electron-electron interactions. The initial (\mathcal{H}_i) and final (\mathcal{H}_f) Hamiltonians, (corresponding to the x-y degrees of freedom) in the presence of a uniform magnetic field in the z direction can therefore be written (using the symmetric gauge for the vector potential \vec{A}) as:

$$\mathcal{H}_{i(f)} = \sum_{k=1}^{N_{i(f)}} \frac{1}{2m^*} \left(\vec{p}_k - \frac{e}{c} \vec{A}(\vec{r}_k) \right)^2 + \frac{1}{2} \sum_{k=1}^M \sum_{l=1}^M \tilde{V}(\vec{r}_k - \vec{r}_l, z_{i(f)}^{k,l}) + \lambda_{i(f)} (\vec{r}_c - \vec{r}_0)^2 , \quad (1)$$

with

$$\vec{A}(\vec{r}) = \frac{1}{2} B \hat{e}_z \times \vec{r} \text{ and,}$$

$$\tilde{V}(\vec{r}, z) = \frac{e^2}{\epsilon_0} \times \left\{ \lim_{\vec{q} \rightarrow 0} \left[\sum_{\vec{R}} \frac{e^{i\vec{q} \cdot \vec{R}}}{|\vec{r} + z\hat{e}_z + \vec{R}|} - \frac{1}{A} \int \frac{d^2 r' e^{i\vec{q} \cdot \vec{r}'}}{|\vec{r} + z\hat{e}_z + \vec{r}'|} \right] - \frac{\theta(\vec{r} + z\hat{e}_z = 0)}{|\vec{r} + z\hat{e}_z|} \right\} ,$$

where

$$\vec{R} = m_1 \vec{a}_1 + m_2 \vec{a}_2, \quad m_{1,2} \in \text{ integers} \quad \text{and} \\ A = |\vec{a}_1 \times \vec{a}_2|.$$

In the above equations, m^* is the effective mass of the electron, ϵ_0 is the dielectric constant of GaAs. $\vec{r}_{i=c}$ corresponds to the electron (which is necessarily one that is *not* pinned) that is recombining with a hole at \vec{r}_0 . The limiting prescription in the expression for $V(\vec{r}, z)$ is for removing the singularity in the lattice sum (the summation over $\{\vec{R}\}$) which is due to the long range nature of the Coulomb interaction.¹⁵ The θ function in this expression is equal to one if the condition in its argument is true and zero otherwise - it allows one to represent a particle to be interacting with its images in other unit cells, but not with itself. $z_{i(f)}^{k,l}$ is the out of plane separation between particles k and l in the initial (final) state. $N_{i(f)}$ is the number of electrons that are dynamical degrees of freedom (in the sense that their coordinates can “evolve”) and M is the total number of electrons including those that are pinned. Hence, in $\mathcal{H}_{i(f)}$, in addition to $\{z_{i(f)}^{k,l}, k, l = 1 \text{ to } M\}$, $\{\vec{r}_k, k = N_{i(f)} + 1 \text{ to } M\}$ also serve only as parameters and not dynamical degrees of freedom. The choice of these parameters varies with the different cases studied here and will be described in detail in the next section. $\lambda_i = 0$ and λ_f is chosen to be a much larger than the “natural” scale (of the same dimension) in this problem: $e^2 n^{1.5} / \epsilon_0$. This choice of λ_f models the experimental situation in which the electron recombines with a screened localized core hole. In principle one would like to remove this recombined electron as a degree of freedom in the final Hamiltonian, but from a calculational point of view it is easier to keep it and introduce the last term in Eq. 1, effectively freezing its motion. The lattice sums in the potential energy terms can be evaluated using standard techniques^{6,16,17} (see Appendix A).

The harmonic approximation to $\mathcal{H}_{i(f)}$ (denoted by $\mathcal{H}_{i(f)}^h$) is developed by expanding the corresponding total potential energy V (=the sum of the last two terms in Eq. 1) about the (classical) equilibrium configurations. The equilibrium configuration is reached by changing the coordinates of all the unpinned electrons such that the forces on them become zero. The coordinates of electrons chosen at the beginning of this “evolution” vary with the different cases studied here and will be described in detail in the next section. The algorithm for this evolution is due to Schweigert and Peeters.¹⁸ This algorithm updates the coordinates by finding the minimum of V when expressed to second order in the coordinate increments *i.e.* if V is expressed as a function of the coordinates of all the unpinned electrons ($q_i, 1 \leq i \leq 2N, N = N_i$ or N_f), then it may be written approximately (V^a), to second order in the coordinate increments from the current position (q_i^t) as:

$$V^a(\mathbf{q}) = V(\mathbf{q}^t) - (\mathbf{f}^t)^T (\mathbf{q} - \mathbf{q}^t) + \frac{1}{2} (\mathbf{q} - \mathbf{q}^t)^T \mathbf{D}^t (\mathbf{q} - \mathbf{q}^t),$$

with

$$(\mathbf{f}^t)^T = - \left[\frac{\partial V(\mathbf{q})}{\partial \mathbf{q}} \right]_{\mathbf{q}=\mathbf{q}^t} \quad \text{and} \quad \mathbf{D}^t = \left[\frac{\partial^2 V(\mathbf{q})}{\partial \mathbf{q} \partial \mathbf{q}^T} \right]_{\mathbf{q}=\mathbf{q}^t},$$

where \mathbf{q} is a column vector whose components are the coordinates q_i and therefore \mathbf{f} becomes a column vector whose components are the forces and \mathbf{D} becomes the (symmetric) dynamical matrix. The lattice sums appearing in \mathbf{f} and \mathbf{D} are again evaluated using standard techniques^{6,16,17} (see Appendix A). The updated coordinate (\mathbf{q}^{t+1}) is determined by minimizing $V^a(\mathbf{q})$. However, far away from the equilibrium configuration the matrix \mathbf{D}^t may not be positive definite and hence $V^a(\mathbf{q})$ may not have a minimum. Therefore the matrix \mathbf{D}^t is (arbitrarily) changed to $\mathbf{D}'^t = \mathbf{D}^t + \eta^t \mathbf{I}$ where η^t is a convergence parameter suitably chosen such that \mathbf{D}'^t is positive definite. We have chosen it to be proportional to the magnitude of the largest component in \mathbf{f}^t . In most cases this modification of \mathbf{D} resulted in a stable evolution. However in some cases it failed *i.e.* \mathbf{D}'^t was nearly singular leading to numerical instabilities. In such cases, \mathbf{D}'^t was more carefully constructed after diagonalizing \mathbf{D}^t : if $\mathbf{D}^t = \mathbf{M} \Lambda \mathbf{M}^T$ (where Λ is the diagonal matrix consisting of the eigenvalues of \mathbf{D}^t) then $\mathbf{D}'^t = \mathbf{M} f(\Lambda) \mathbf{M}^T$ such that $f(\Lambda)$ is a diagonal positive definite matrix with the function f chosen to satisfy $f(\Lambda) \rightarrow \Lambda$ as convergence is reached. Hence the algorithm for updating the coordinates becomes:

$$\mathbf{q}^{t+1} = \mathbf{q}^t + (\mathbf{D}'^t)^{-1} \mathbf{f}^t.$$

The above algorithm is iterated until convergence is reached - the root mean squared force per electron becoming smaller than a chosen value. This yields the equilibrium configuration \mathbf{q}^{eq} .

The process of determining the equilibrium configuration provides all the necessary parameters (from the potential energy terms) for the harmonic approximation to the Hamiltonian. In this approximation the potential V is replaced by its approximate form $V^a(\mathbf{q})$, with the expansion of $V^a(\mathbf{q})$ around the equilibrium configuration \mathbf{q}^{eq} . Hence, since $\mathbf{f}^{eq} = 0$, the parameters that enter the approximate Hamiltonian are contained in the dynamical matrix \mathbf{D}^{eq} . This matrix is positive definite since the equilibrium configuration reached is *stable*. There are no modes corresponding to neutral equilibrium since global translational invariance is broken by the pinned electrons. There is no global rotational invariance even in the absence of pinning due to the chosen periodic boundary conditions. Further, due to the linear variation of the vector potential $A(\vec{r})$ with \vec{r} , the approximated initial (\mathcal{H}_i^h) and final Hamiltonians (\mathcal{H}_f^h) can be written (with $\epsilon_{i(f)}^m = V(\mathbf{q}_{i(f)}^{eq})$) as:

$$\mathcal{H}_{i(f)}^h = \frac{1}{2m^*} (\mathbf{\Pi} - \mathbf{B}\mathbf{q})^T (\mathbf{\Pi} - \mathbf{B}\mathbf{q}) \\ + \frac{1}{2} (\mathbf{q} - \mathbf{q}_{i(f)}^{eq})^T \mathbf{D}_{i(f)}^{eq} (\mathbf{q} - \mathbf{q}_{i(f)}^{eq}) + \epsilon_{i(f)}^m, \quad (2)$$

where $\mathbf{\Pi}$ is a column vector whose components Π_k are the (canonical) momenta corresponding respectively to the coordinates q_k ($1 \leq k \leq 2N_f$) and \mathbf{B} is a (antisymmetric) matrix corresponding to the vector potential. Note that the harmonically approximated Hamiltonians have an equal number of dynamical degrees of freedom ($2N_f$). For the disordered systems investigated, in some cases we chose to randomly pin a small number of electrons after the initial equilibrium configuration had been found. This is meant to roughly model the effect of pinned in-plane charged impurities²¹ that are not due to the charged acceptors. In such cases $N_f < N_i$.

Gauge freedom may now be exploited to change $\vec{A}(\vec{r}_k)$ to the form $\vec{A}(\vec{r}_k) = \frac{1}{2}B\hat{e}_z \times (\vec{r}_k - (\vec{r}_k)_i^{eq})$ where $(\vec{r}_k)_i^{eq}$ corresponds to the equilibrium configuration \mathbf{q}_i^{eq} of the initial Hamiltonian. Further defining $\Phi_i = \mathbf{q} - \mathbf{q}_i^{eq}$, $\Phi_f = \mathbf{q} - \mathbf{q}_f^{eq}$, and the corresponding canonical momenta $\mathbf{\Pi}_i = \mathbf{\Pi}$, $\mathbf{\Pi}_f = \mathbf{\Pi} - \mathbf{B}(\mathbf{q}_i^{eq} - \mathbf{q}_f^{eq})$, \mathcal{H}_i^h and \mathcal{H}_f^h may be written as:

$$\mathcal{H}_{i(f)}^h = \epsilon_{i(f)}^m + \frac{1}{2m^*} \times \begin{bmatrix} \Phi_{i(f)}^T \Pi_{i(f)}^T \\ \mathbf{0} \end{bmatrix} \begin{bmatrix} m^* \mathbf{D}_{i(f)}^{eq} + \mathbf{B}^T \mathbf{B} & -\mathbf{B}^T \\ -\mathbf{B} & \mathbf{I} \end{bmatrix} \begin{bmatrix} \Phi_{i(f)} \\ \Pi_{i(f)} \end{bmatrix},$$

with

$$\begin{bmatrix} \Phi_f \\ \Pi_f \end{bmatrix} = \begin{bmatrix} \Phi_i \\ \Pi_i \end{bmatrix} + \begin{bmatrix} \mathbf{I} & -\mathbf{I} \\ \mathbf{B} & -\mathbf{B} \end{bmatrix} \begin{bmatrix} \mathbf{q}_i^{eq} \\ \mathbf{q}_f^{eq} \end{bmatrix}. \quad (3)$$

The harmonic Hamiltonians thus developed can be considered to be functions of classical variables or the corresponding quantum mechanical operators (with electrons being spinless). In either case, by a linear canonical transformation of the phase space variables, they can be written as a sum of uncoupled (normal) modes (see Appendix B). Hence

$$\mathcal{H}_{i(f)}^h = \epsilon_{i(f)}^m + \frac{1}{2} \begin{bmatrix} \Psi_{i(f)}^T \Xi_{i(f)}^T \\ \mathbf{0} \end{bmatrix} \begin{bmatrix} \Omega_{i(f)} & \mathbf{0} \\ \mathbf{0} & \Omega_{i(f)} \end{bmatrix} \begin{bmatrix} \Psi_{i(f)} \\ \Xi_{i(f)} \end{bmatrix}, \quad (4)$$

$$\text{with } \begin{bmatrix} \Psi_{i(f)} \\ \Xi_{i(f)} \end{bmatrix} = [\mathbf{C}_{i(f)}] \begin{bmatrix} \Phi_{i(f)} \\ \Pi_{i(f)} \end{bmatrix}. \quad (5)$$

Since the transformation \mathbf{C}_i (\mathbf{C}_f) is canonical, the components of Ξ_i (Ξ_f) are the conjugate momenta corresponding to the components of the Ψ_i (Ψ_f) with Ω_i (Ω_f) being a diagonal matrix consisting of the normal mode frequencies of \mathcal{H}_i^h (\mathcal{H}_f^h).

The Planck's constant \hbar may now be explicitly introduced into the Hamiltonians $\mathcal{H}_{i(f)}$ by assuming that $\Xi_{i(f)}$ and $\Psi_{i(f)}$ are quantum mechanical operators. Hence, defining the column vectors consisting of lowering ($\mathbf{a}_{i(f)}$) and raising ($\mathbf{a}_{i(f)}^\dagger$) operators:

$$\begin{bmatrix} \mathbf{a}_{i(f)} \\ \mathbf{a}_{i(f)}^\dagger \end{bmatrix} = \left(\frac{1}{2\hbar}\right)^{\frac{1}{2}} \begin{bmatrix} \mathbf{I} & -i\mathbf{I} \\ \mathbf{I} & -i\mathbf{I} \end{bmatrix} \begin{bmatrix} \Psi_{i(f)} \\ \Xi_{i(f)} \end{bmatrix}, \quad (6)$$

the Hamiltonians may be written as

$$\mathcal{H}_{i(f)}^h = \epsilon_{i(f)}^m + \frac{\hbar}{2} \begin{bmatrix} \tilde{\mathbf{a}}_{i(f)} \tilde{\mathbf{a}}_{i(f)}^\dagger \end{bmatrix} \begin{bmatrix} \mathbf{0} & \Omega_{i(f)} \\ \Omega_{i(f)} & \mathbf{0} \end{bmatrix} \begin{bmatrix} \mathbf{a}_{i(f)} \\ \mathbf{a}_{i(f)}^\dagger \end{bmatrix}, \quad (7)$$

with (using Eqs. 3,5 and 6)

$$\begin{bmatrix} \mathbf{a}_f \\ \mathbf{a}_f^\dagger \end{bmatrix} = \mathbf{T} \begin{bmatrix} \mathbf{a}_i \\ \mathbf{a}_i^\dagger \end{bmatrix} + \mathbf{w}, \quad (8)$$

where \mathbf{T} is a matrix of the form

$$\mathbf{T} = \begin{bmatrix} \mathbf{U} & \mathbf{V} \\ \mathbf{V}^* & \mathbf{U}^* \end{bmatrix} = \frac{1}{2} \begin{bmatrix} \mathbf{I} & i\mathbf{I} \\ \mathbf{I} & -i\mathbf{I} \end{bmatrix} \mathbf{C}_f \mathbf{C}_i^{-1} \begin{bmatrix} \mathbf{I} & \mathbf{I} \\ -i\mathbf{I} & i\mathbf{I} \end{bmatrix}, \quad (9)$$

and \mathbf{w} is a vector of the form

$$\begin{aligned} \mathbf{w} &= \begin{bmatrix} \Delta \\ \Delta^* \end{bmatrix} \\ &= \left(\frac{1}{2\hbar}\right)^{\frac{1}{2}} \begin{bmatrix} \mathbf{I} & i\mathbf{I} \\ \mathbf{I} & -i\mathbf{I} \end{bmatrix} \mathbf{C}_f \begin{bmatrix} \mathbf{I} & -\mathbf{I} \\ \mathbf{B} & -\mathbf{B} \end{bmatrix} \begin{bmatrix} \mathbf{q}_i^{eq} \\ \mathbf{q}_f^{eq} \end{bmatrix}. \end{aligned} \quad (10)$$

We now proceed to describe the theory of PL. The initial states $|\psi_i\rangle$ are assumed to be eigenstates of \mathcal{H}_i^h (with $\mathcal{H}_i^h|\psi_i\rangle = E_i|\psi_i\rangle$) whose distribution is determined by the temperature $\beta = (k_b T)^{-1}$. After the sudden perturbation, in which the Hamiltonian changes from \mathcal{H}_i^h to \mathcal{H}_f^h , the initial state is assumed to collapse into a final state that is an eigenstate $|\psi_f\rangle$ of \mathcal{H}_f^h (with $\mathcal{H}_f^h|\psi_f\rangle = E_f|\psi_f\rangle$) with a probability $|\langle\psi_f|\psi_i\rangle|^2$. In this process a photon of frequency ω is emitted. Assuming conservation of energy across the sudden perturbation, $\hbar\omega = E_i - E_f$. Hence the probability density of the photon frequency $\mathcal{P}(\omega)$ is given by:

$$\mathcal{P}(\omega) = \left[\sum_i e^{-\beta E_i} \right]^{-1} \sum_i e^{-\beta E_i} \sum_f |\langle\psi_f|\psi_i\rangle|^2 \delta(\hbar^{-1}(E_i - E_f) - \omega). \quad (11)$$

$\mathcal{P}(\omega)$ may be calculated from its Fourier transform $\tilde{\mathcal{P}}(t)$:

$$\mathcal{P}(\omega) = \frac{1}{2\pi} \int_{-\infty}^{+\infty} dt e^{-i\omega t} \tilde{\mathcal{P}}(t), \quad (12)$$

with $\tilde{\mathcal{P}}(t)$ given by (inverting Eq. 12 and using Eq. 11):

$$\tilde{\mathcal{P}}(t) = \frac{\sum_i e^{-\beta E_i} \sum_f |\langle\psi_f|\psi_i\rangle|^2 e^{i\hbar^{-1}(E_i - E_f)t}}{\sum_i e^{-\beta E_i}}. \quad (13)$$

Rewriting Eq. 13 using the Hamiltonians $\mathcal{H}_{i(f)}^h$:

$$\tilde{\mathcal{P}}(t) = \left[\sum_i \langle \psi_i | e^{-\beta \mathcal{H}_i} | \psi_i \rangle \right]^{-1} \times \sum_i \langle \psi_i | \sum_f | \psi_f \rangle \langle \psi_f | e^{-i\hbar^{-1} \mathcal{H}_f^h t} e^{i\hbar^{-1} \mathcal{H}_i^h (t + i\hbar\beta)} | \psi_i \rangle. \quad (14)$$

Since $|\psi_i\rangle$ and $|\psi_f\rangle$ constitute an orthonormal bases, Eq. 14 may be written in terms of trace (Tr) operations that are basis independent:

$$\tilde{\mathcal{P}}(t) = \frac{Tr \left[e^{-i\hbar^{-1} \mathcal{H}_f^h t} e^{i\hbar^{-1} \mathcal{H}_i^h (t + i\hbar\beta)} \right]}{Tr \left[e^{-\beta \mathcal{H}_i} \right]}. \quad (15)$$

$\mathcal{P}(\omega)$ is then computed using Eq. 12. In order to compare $\mathcal{P}(\omega)$ to the experimental line shape of the intensity $I(\omega)$ we make the final assumption that:

$$I(\omega) \propto \mathcal{P}(\omega). \quad (16)$$

The above relationship (after substituting for $\mathcal{P}(\omega)$ using Eq. 11) may be derived using first order time dependent perturbation theory with a time independent Hamiltonian that includes the photon degrees of freedom together with the z degree of freedom for the recombining electron (see Appendix C). Finally, we note that our model for the final state of the recombined electron formally retains it as a degree of freedom, albeit with a very large spring constant λ_f . In practice this means that the spectrum $\mathcal{P}(\omega)$ consists of a series of highly separated peaks, each corresponding to a different state of the recombined electron plus phonons in the remaining lattice. Physically, only the state in which the electron is most strongly localized at the location of the core hole - *i.e.*, the lowest energy state of the harmonic potential due to the λ_f in Eq. 1 - is truly relevant. Because of the separation of energy scales between the “ λ modes” and the lattice phonon modes, one may easily identify the highest energy peak in $\mathcal{P}(\omega)$ as the experimentally relevant spectrum. From a computational point of view, one would like to eliminate the other peaks, as they are unphysical and can consume much cpu time in their computation. This can be accomplished by introducing an imaginary component *i.e.*, a broadening to the normal mode frequencies. The precise way in which this is done, along with several other practical issues in our computation and approximation scheme, is discussed in Appendix D. Details of the computation of the traces appearing in Eq. 15 are given in Appendix E.

III. RESULTS AND DISCUSSION

We now present our theoretical results corresponding to the experiment of Kukushkin *et al*⁸ who identify a particular “late time” spectrum in their time resolved PL

spectra as corresponding to the recombination of electrons from a Wigner solid with holes bound to acceptor atoms a certain distance away from the 2DES. For comparing our calculations with their observations, we set the electron density n to $5.3 \times 10^{10}/\text{cm}^2$, the filling factor ν to 0.1337 (a magnetic field $B \approx 16.4$ Tesla), the temperature T to 45 mK and the distance between the 2DES and the acceptor atoms (z_0) to 300 Å. The effective mass parameter m^* is set to $0.068m_e$ and the dielectric constant ϵ_0 is set to 12.8 which correspond to the AlGaAs-GaAs heterostructure. We adopt natural units defined by n , e^2/ϵ_0 and m^* . Therefore the natural length scale is ($= 1/\sqrt{n}$) ≈ 434 Å, the natural frequency scale is ($= \sqrt{e^2 n^{1.5}/\epsilon_0 m^*}$) ≈ 1.88 THz and the natural energy scale is ($= e^2 n^{0.5}/\epsilon_0$) ≈ 2.59 meV. In these units, the cyclotron frequency ≈ 22.5 , $\hbar \approx 0.479$ and the inverse temperature (β) ≈ 668 .

It must be noted that the experimental late time spectral “width”⁸ (the range of photon *frequencies* for which the intensity can be distinguished from being ≈ 0) is ~ 3.0 in the natural units chosen. We study four cases here in an attempt to reproduce this width and thereby identify the experimentally relevant one. In one of these cases we also attempt to give an alternative interpretation to the experimental observation⁸ of a “double peak” during continuous illumination. As the experimental spectra have the intensity plotted against increasing photon wavelength,⁸ we show the calculated spectra with decreasing photon frequency. The comparison of line shape can then be directly made since in the experiment the spread in photon frequency is a very small fraction ($\sim 2 \times 10^{-3}$) of the average frequency. As mentioned previously, the binding energy of the electron to the hole, which determines the position of the spectrum along the frequency axis, cannot be determined in our model and has been set to zero when presenting the results. Therefore the calculated peak always appears in the negative frequency domain.

A. Perfect Wigner lattice with Coulomb interactions

In this case the initial (classical) equilibrium configuration corresponds to a perfect triangular lattice. Because of the translational invariance of a perfect, unpinned Wigner crystal, one cannot apply the harmonic approximation consistently to this case: the sudden change in potential will introduce a large coherent motion of the center of mass in the subsequent dynamics of the system. This behavior is unphysical, because in practice a Wigner crystal will always be pinned by disorder. We therefore assume that the electrons at the boundary of our supercell are actually pinned, and are not dynamical degrees of freedom. This allows the harmonic approximation to be applied consistently. We will show below that the PL spectrum converges rapidly as the system size increases, so that the pinning at the boundary does

not affect our final results.

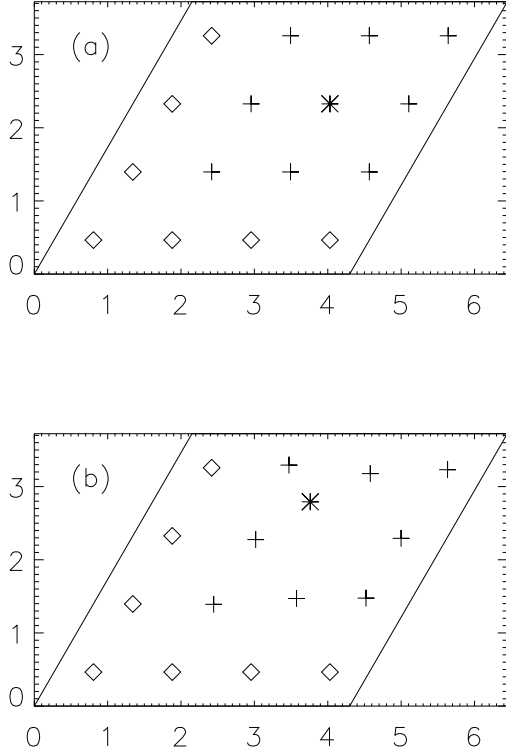


FIG. 1. Equilibrium x - y configuration of the perfect Wigner lattice (a) corresponding to the initial Hamiltonian \mathcal{H}_i (Eq. 1) and the same of the perturbed lattice (b) corresponding to the final Hamiltonian \mathcal{H}_f . Pinned and unpinned electrons are shown by \diamond and $+$ respectively. The figures correspond to the case when the number of unpinned electrons $N_i = N_f = 9$ with the total number of electrons $M = 16$. The “central” (unpinned) electron is shown by $*$. The axes are labeled in units of the natural length scale of the problem: (total electron density) $^{-1/2}$.

Here, all the electrons interact through the “ideal” Coulomb interaction. The initial configuration can therefore be directly constructed by laying down the electrons at lattice positions or arrived at by evolving an initial configuration in which only the pinned electrons are laid down at lattice positions with the rest of the electrons being randomly placed. The final configuration, obtained through evolution beginning with the perfect Wigner lattice, corresponds to confining the “central” electron (see Fig. 1) to *one particular* point on the boundary of its Wigner-Seitz cell (corresponding to the perfect lattice). This choice is motivated by the interpretation⁸ that the late time PL spectrum corresponds to recombination events in which the distance between the hole (bound to the acceptor) and the recombining electron is maximal. It must be noted that to determine the final equilibrium configuration it is not appropriate to begin with a random configuration of unpinned electrons since then the equilibrium configuration reached may involve exchanges of electrons with respect to the perfect lattice.

In this work, we assume that the initial state [Fig. 1(a)] may be regarded as a deformation of a classical equilibrium that is closest in configuration to this state [Fig. 1(b)], and that the subsequent motion of the electrons is due to the vibrations around the latter state. While final states in which electrons are exchanged are in principle relevant, such exchanges in practice contribute little to the PL spectrum.¹⁹

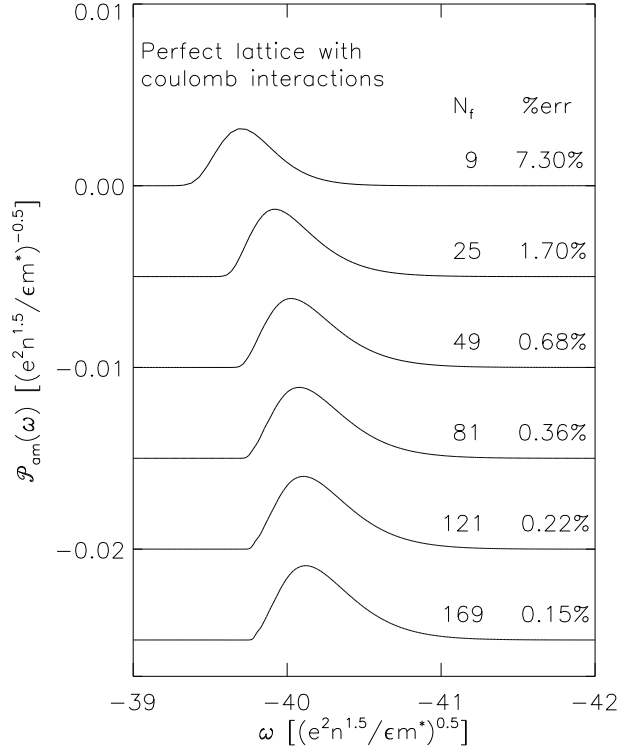


FIG. 2. Calculated spectra from transitions similar to that in Fig. 1 (which corresponds to the number of unpinned electrons (N_f) being equal to nine). For each value of N_f , flat regions correspond to the zero of $\mathcal{P}_{am}(\omega)$. $\%err$ is the increase in calculated spectral width due to approximations made to get a continuous curve for the finite N_f . The spectral width saturates (around $N_f = 25$) to $\sim \frac{1}{3}$ of that observed by Kukushkin *et al.*² However, a qualitative feature of the experimental spectrum is present in the theoretical results: a faster rising edge as compared to the falling edge.

We can therefore fix the parameters in $\mathcal{H}_{i(f)}$ (Eq. 1): $N_i = N_f = P^2$, $M = (P+1)^2$ (Fig. 1 corresponds to the case when $P = 3$), $z_i^{k,l} = 0$ (corresponding to all electrons initially being in the x - y plane) and $z_f^{k,l} = z_0(\delta_{l,c} - \delta_{k,c})$ (corresponding to all the electrons finally being in the x - y plane except for the central electron c being below the plane at the position of the acceptor atoms). \vec{r}_0 and other parameters corresponding to the x - y position of the pinned electrons (\vec{r}_i , $i = N_{i(f)} + 1$ to M) can be inferred from Fig. 1. We have studied the cases with $P = [3, 5, 7, 9, 11, 13]$. In each of these cases we have chosen the parameter Γ_0 (a broadening parameter intro-

duced to make the phonon density of states continuous; see Appendix D) to be equal to the smallest phonon frequency in \mathcal{H}_i^h . These values (in units of $\sqrt{e^2 n^{1.5} / \epsilon_0 m^*}$) are $[7.59, 4.49, 3.08, 2.30, 1.82, 1.49] \times 10^{-2}$ (corresponding to the cases with $P = [3, 5, 7, 9, 11, 13]$ respectively). It must be noted that all the electrons including the pinned ones are included in the computation of the density n .

Fig. 2 shows the calculated spectra. The error in the spectral width is due to the approximation of replacing the delta function in Eq.11 by a Gaussian of width Γ_0 . Note that the spectral width seems to have saturated beyond $N_f \approx 25$ but it is only $\sim 1/3$ of that experimentally observed.⁸ A qualitative feature of the experimental spectrum is however reproduced: a faster rising edge as compared to the falling edge.

B. Perfect Wigner lattice with softened Coulomb interactions

We now soften all the in-plane electron interactions in an attempt to see if it results in a broader spectrum than the previous case. The softened interaction is of the form $1/\sqrt{r^2 + \bar{z}_0^2}$. \bar{z}_0 is chosen to be 150\AA - a significant fraction of the inter-electron distance. This form of the interactions is motivated by the fact that the electrons are not strictly confined to two dimensions at the interface of the GaAs-AlGaAs heterostructure, there is a finite extent in the z direction of the wavefunction confining the 2DES. This particularly simple form of the Coulomb interaction incorporating the finite width of the electron layer has been quantitatively successful in obtaining the fractional quantum Hall excitation gap energies in the 2DES,²⁰ which motivates us to apply this softened interaction in the Wigner crystal PL calculation. The procedure to obtain the initial and final equilibrium configurations remains the same as before. These configurations are similar to that shown in Fig. 1 - there being a “wall” of pinned electrons on the boundary. Only one system size is studied with $N_{i(f)} = 7^2$, $M = 8^2$, $z_i^{k,l} = \bar{z}_0(1 - \delta_{k,l})$ and $z_f^{k,l} = \bar{z}_0(1 - \delta_{k,l}) + (z_0 - \bar{z}_0)|\delta_{k,c} - \delta_{l,c}|$ where c again corresponds to the central electron. The parameters \vec{r}_0 and $\{\vec{r}_i, i = N_{i(f)} + 1 \text{ to } M\}$ can be inferred from Fig. 1. Again, Γ_0 has been chosen to be the smallest phonon frequency of \mathcal{H}_i^h ($= 2.52 \times 10^{-2} \sqrt{e^2 n^{1.5} / \epsilon_0 m^*}$).

Fig. 3 shows the calculated spectrum. The width is slightly reduced (still roughly $1/3$ of the experimental value) as compared to the case with ideal Coulomb interactions. This can be attributed to a faster falling edge making it less similar to the experimental spectrum.⁸ We conclude that only softening the Coulomb interaction by the finite layer thickness of the 2DES cannot account for the experimental spectral width. This is understandable, because the spectral width of the PL spectrum is primarily determined by the physics of the recombination process at the acceptor sites and not by the details of the electron-electron interaction.

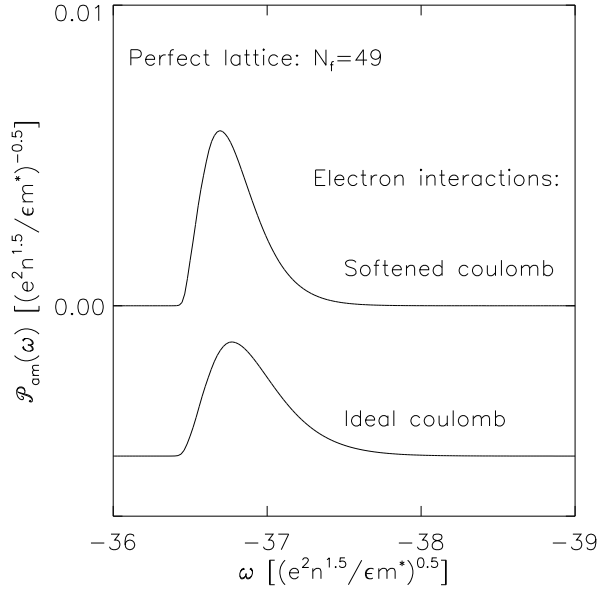


FIG. 3. Calculated spectrum from transition similar to that in Fig. 1 (which corresponds to the number of unpinned electrons N_f being equal to nine) with softened Coulomb interaction. For comparison the spectrum corresponding to ideal Coulomb electron interaction is included. It has been shifted to the left to make the photon energy corresponding to the difference in the ground state energies coincide with the same point of the first curve. Softening the electron interactions results in the spectrum being less similar to the experimental curve: the width is slightly reduced (continues to be $\sim 1/3$ of the experimental value.) and it has a faster falling edge.

C. Perfect Wigner lattice with recombination position averaging

Since the “softened” Coulomb interaction does not lead to any improvement in the agreement between theory and experiment, we now revert back to “ideal” Coulomb interaction for in-plane electrons and consider averaging spectra corresponding to different x - y positions of the recombination center (\equiv acceptor atom position) relative to the initial position of the recombining electron. The averaging is carried out assuming that the x - y distribution of acceptor atoms is uniform. This results in a uniform distribution for the position of the recombination center within the Wigner-Seitz cell of the recombining electron. It models the situation for which the PL is not time resolved,^{8,10} so that no particular final position of the recombining electron is favored. Symmetries can be exploited to reduce the actual region of the Wigner-Seitz cell that needs to be explored. For configurations of the type shown in Fig. 1 (a), due to the presence of the “wall” of pinned electrons on the boundary, there are

only two reflection symmetries (each along a diagonal of the system) for the recombination positions corresponding to the central electron. Therefore, to get the average spectrum, $1/4$ the area of the Wigner-Seitz cell needs to be explored. However, if there was a hexagonal boundary of pinned electrons around the recombining electron then there would be six-fold together with reflection symmetries along the diagonals which would reduce the region needed to be explored to $1/12$ the area of the Wigner-Seitz cell. We therefore consider such a configuration (Fig. 4).

they are included in the computation of the total energy - one third of which is the actual energy of the hexagonal system. During evolution, the forces and the dynamical matrix need to be computed corresponding to only the unpinned electrons within *any one* hexagon (interactions between all inequivalent electrons are taken into account). By symmetry they are the same for the corresponding unpinned electrons in the other two hexagons. The displacements are therefore computed for only one set of unpinned electrons but it is applied to all the unpinned electrons thus preserving the equivalence

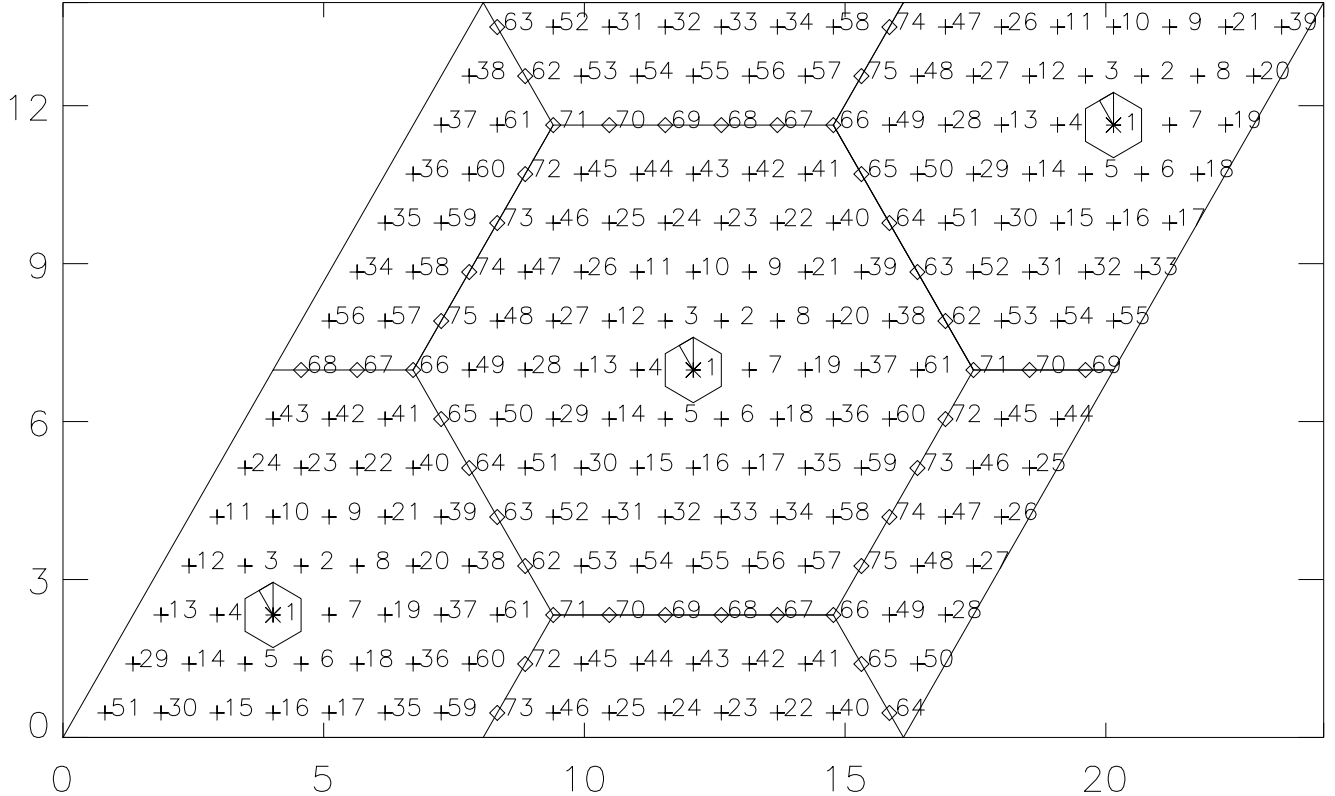


FIG. 4. The figure shows the initial equilibrium configuration of the system with a hexagonal wall of pinned electrons. Electrons with the same number are considered equivalent. This, in addition to application of periodic boundary conditions about the parallelogram, results in the hexagonal system being repeated periodically - three copies of which are embedded in the parallelogram. Therefore the Wigner-Seitz cell of the “central” recombining electron (numbered 1) has all the symmetries of a triangular lattice. This reduces the region of different recombination positions to be explored to $\frac{1}{12}$ the area of the Wigner-Seitz cell - the triangle within the hexagon around the electron numbered 1.

Fig. 4 shows the construction of the system with a hexagonal wall of pinned electrons. Three such copies are needed for embedding into a parallelogram - then the usual periodic boundary conditions about the parallelogram results in the periodic repetition of the hexagonal system. The initial equilibrium configuration is directly constructed as it corresponds to a perfect triangular lattice. The final equilibrium configuration is arrived at through evolution beginning with this configuration. However, as electrons with the same number (see Fig. 4) are considered equivalent, the corresponding "self interaction" terms are neglected during the computation of the forces and the dynamical matrix. Nevertheless,

of the electrons with same number through the evolution. The parameters in $\mathcal{H}_{i(f)}$ used are: $N_i = N_f = 61$, $M = 75$, $z_i^{k,l} = 0$, $z_f^{k,l} = z_0(\delta_{k,1} - \delta_{l,1})$. The parameters \vec{r}_i , $i = N_{i(f)} + 1$ to M can be inferred from Fig. 4.

PL spectra are computed for different recombination positions (the parameter r_0 in Eq. 1) of the electron numbered 1 (see Fig. 4). Each of the spectra is computed with Γ_0 being equal to the smallest phonon frequency of $\mathcal{H}_i^h: = 3.46 \times 10^{-2} \sqrt{e^2 n^{1.5} / \epsilon_0 m^*}$. Fig. 5 shows their variation for recombination positions distributed uniformly along the edge of the Wigner-Seitz cell. Although the overall normalization increases rapidly with decreasing

distance of the recombination center from the initial position of electron 1, the position of the peak shifts only slightly to the left. Hence the average of these spectra continues to have the typical width of each curve: $\sim 1/3$ of that observed in time resolved PL.⁸

The average PL spectrum - using 127 distinct points uniformly distributed in the Wigner-Seitz cell - is shown as an inset to Fig. 5. The spectrum is relatively narrow, and is in fact dominated by PL from recombination events in which the x - y motion of the electron is quite small. This is expected as it reflects the fact that the overlap between the recombining electron's initial and final states falls off rapidly as a function of its displacement. The spectrum is much narrower than seen in experiment, and does not reflect the experimentally observed double peak structure.^{8,10} The latter has been interpreted as evidence of liquid-solid coexistence due to disorder and/or finite temperatures,^{8,10,14} and our present results implicitly agree with this interpretation - a model of a perfect uniform solid as used in our work cannot explain the structure seen in continuous wave experiments.

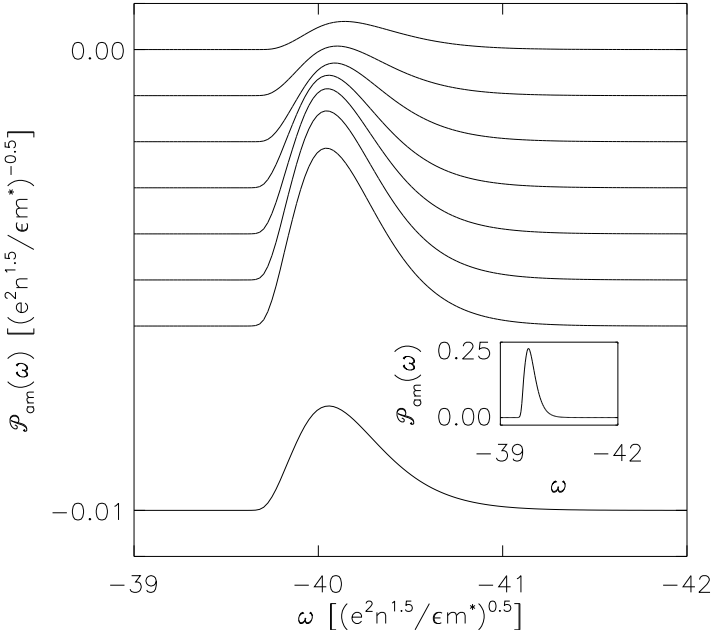


FIG. 5. Spectra for recombination positions uniformly distributed along the edge of the Wigner-Seitz cell (see Fig. 4). They are shown in the order of decreasing distance from the initial position of the recombining electron. The final spectrum is the average of these spectra. It continues to have a width that is $\frac{1}{3}$ of that in experiment.⁸ The inset shows the average spectrum corresponding to points distributed uniformly over the entire Wigner-Seitz cell (its axes are in the same units as the figure). It is dominated by the spectra corresponding to recombination positions close to the initial position of the recombining electron.

D. Wigner lattice with disorder averaging

We finally consider a disordered system (again with ideal Coulomb interactions) in which the disorder is due to pinned electrons below the x - y plane corresponding to charged acceptor atoms *i.e.* we assume that the spectrum of interest corresponds to a time when most of the recombination events have occurred so that all the acceptor atoms are charged in equilibrium. We consider a system size of 64 (initially) in-plane electrons. Unlike the previous cases, only these electrons are included in the computation of the density n . As the experimental density of acceptor atoms⁸ is $5 \times 10^9/\text{cm}^2$ the number of charged acceptor atoms corresponding to 64 in-plane electrons must be very nearly 6. We therefore have 5 pinned electrons below the x - y plane corresponding to these atoms - the sixth would correspond to the recombination event for which the spectrum is computed.

In the absence any concrete information about the correlations between different acceptor atom coordinates that exist due to the process of δ doping we have assumed that each acceptor atom's x - y position is uniformly randomly distributed and is independent of any other acceptor atom's position. Therefore the 5 pinned electrons are independently placed randomly in the system. In principle, one would like to find the point farthest from all the electrons for a given disorder realization, and, since acceptors located near such points are least likely to have a recombination event, assume that the late-time PL spectrum is dominated by an acceptor at this point. In practice, rather than generate a large number of disorder realizations, we choose just one, construct the Wigner-Seitz cells for the disordered system, and choose the corners of these cells as candidates for late-time PL recombination events. We believe this procedure will produce spectra qualitatively and even quantitatively close to that found by direct disorder-averaging, and is numerically much less time consuming. Essentially, we are assuming the system self-averages. To model the likelihood that a particular corner-configuration is likely to be available in the late-time spectroscopy, we additionally introduce a weighting factor for each corner. We do this by constructing the Voronoi cell around the lattice of corners, and set the weight for the corner to be proportional to its dual cell's area. Thus, acceptors that are particularly far from electrons are more likely to be available for PL events after long-time, and are given somewhat larger weights.

Two cases are studied here: Case (a) - None of the 64 in-plane electrons are pinned, Case (b) - Two of the in-plane electrons that are maximally distant (as measured in the x - y plane) from the pinned electrons are additionally pinned *after* obtaining the initial equilibrium configuration (electrons numbered 13 and 47 in Fig. 6). The latter case is chosen to study what effects in-plane pinned electrons²¹ could have on the PL. As will be seen below, their effect is quite small. The parameters of $\mathcal{H}_{i(f)}$ (Eq. 1) can therefore be set to: $N_i = 64$, $N_f = 64$ for case (a)

and 62 for case (b), $M = 69$, $z_i^{k,l} = z_0(\delta_{k,\geq 65} - \delta_{l,\geq 65})$, $z_f^{k,l} = z_0(\delta_{k,\geq 65} + \delta_{k,c} - \delta_{l,\geq 65} - \delta_{l,c})$ where c corresponds to the recombining electron. The parameters \vec{r}_i , $i = N_{i(f)} + 1$ to M can be inferred from Fig. 6.

The initial equilibrium configuration is reached through evolution beginning with a random distribution of the in-plane electrons. Beginning with this configuration, the final equilibrium configuration is reached in ten steps - each step localizing the recombining electron (through the choice of the parameter \vec{r}_0 in Eq. 1) closer to its final position which is chosen to be one of the corners of the Voronoi cell that initially contained the electron (see Fig. 6). This procedure allows us to find the closest minimum energy state in configuration space.

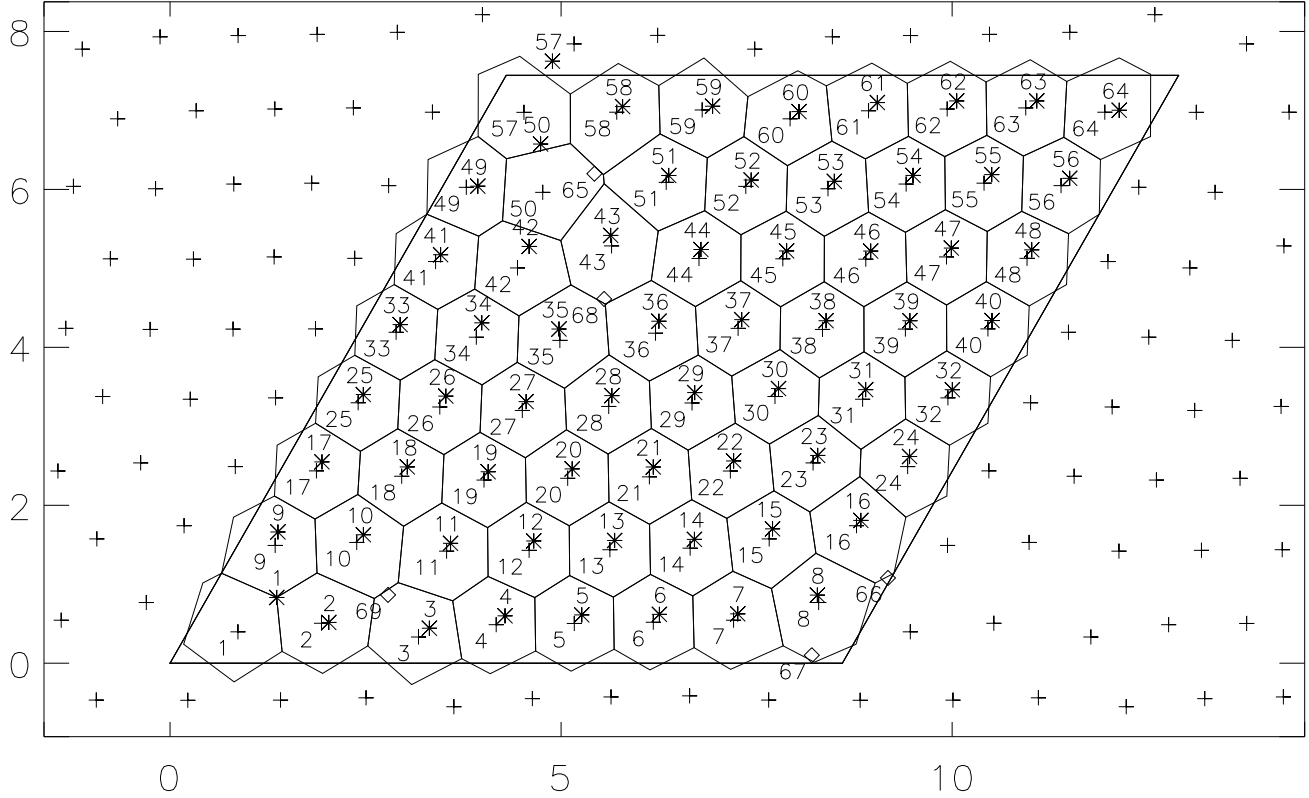


FIG. 6. The figure shows the initial equilibrium configuration of unpinned electrons (marked by '+') and a particular final configuration of electrons (marked by '*') corresponding to the recombination of the electron numbered 1 with a bound hole at a corner of the Voronoi cell that contained this electron. For easy visualization of the Voronoi cells, the initial configuration has been shown to be periodically repeated. Electrons that have already recombined are represented as pinned electrons (marked by \diamond and numbered 65 through 69) that are independently and randomly placed in the system. They are not considered in the Voronoi construction.

It appears that the width of the average spectra corresponding to the two cases studied is mainly due to the wide distribution ($D(\omega_p)$) of the position of the peak (ω_p) in the individual spectra that constitute the average. This distribution is constructed by binning the peak positions into intervals in frequency. All peaks within a bin *do not* contribute equally to the distribution height - each contributes in proportion to the product of the corresponding Voronoi corner area and the area un-

der the corresponding spectrum ($= \tilde{\mathcal{P}}_{am}(t = 0)$). Fig. 7 shows the normalized distributions for the two cases studied here. It may be seen that they have a width of $\sim 7\sqrt{e^2 n^{1.5}/\epsilon_0 m^*}$. The insets show the corresponding distributions for a *second disorder realization* - they are similar in shape but have a somewhat smaller width: $\sim 5\sqrt{e^2 n^{1.5}/\epsilon_0 m^*}$. We therefore expect that the average spectra corresponding to the first disorder realization to be roughly similar to the true disorder averaged spectra.

The individual spectra in the average spectrum corresponding to the two cases studied here have been computed using $\Gamma_0 = 3.80 \times 10^{-2} \sqrt{e^2 n^{1.5}/\epsilon_0 m^*}$ - the smallest non-zero phonon frequency of the perfect unpinned lattice with 64 electrons. Fig. 8 shows these average

spectra. As expected they are have a very large ($> 7\sqrt{e^2 n^{1.5}/\epsilon_0 m^*}$) width: $\sim 9\sqrt{e^2 n^{1.5}/\epsilon_0 m^*}$. This is ~ 3 times the experimental value.⁸ The extra broadening seen in Fig. 8 over that of Fig. 7 is due to the shakeup of phonons.

We speculate that the disagreement in these results and those found in experiment may be due to an overestimate of the disorder strength assumed in our uncorrelated random disorder model. In particular, the as-

sumption that nearly all the holes on acceptor atoms have recombined with electrons would be true only after very long waiting times, and it is unclear that this limit is actually achieved in experiment.⁸ Subsequent measurements⁷ have suggested that it may indeed be the case that longer waiting times are needed. Clearly, one could “tune” the level of disorder in our model to obtain the experimentally observed linewidth. However, this would require a painstaking and somewhat artificial “fine-tuning” of our model. An independent measurement of the density of charged acceptors in these systems in the late time PL would greatly facilitate a quantitative comparison of this model with experiment. In this context it is worthwhile to point out that in general modulation δ -doped heterostructures are known²² to have substantial correlation among the impurity sites, and an uncorrelated random disorder model overestimates the disorder strength producing lower electron mobilities than experimentally observed. Any such correlation among the acceptor sites in our problem would reduce the spectral width of our calculated PL spectra, bringing experiment and theory into closer quantitative agreement.

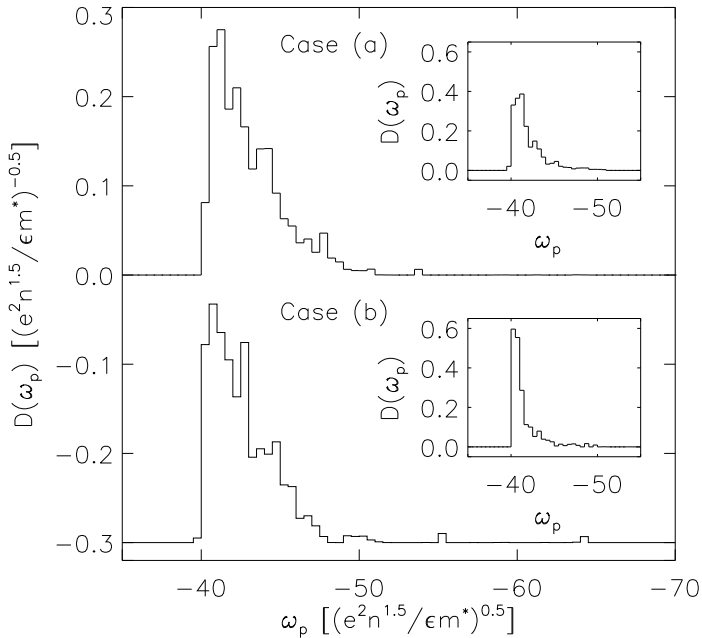


FIG. 7. The figure shows the distribution of peak positions (extended flat regions correspond to its zero value) in the spectra corresponding to the disorder realization shown in Fig. 6 for the two cases: (a) with no in-plane pinning centers and (b) with two in-plane pinning centers. The broad distributions imply that the corresponding average spectra must be at least as wide. The insets (whose axes are labeled in the same units as the figure) show the corresponding distributions for a second disorder realization. They are similar those of the first but have a slightly smaller width. This suggests that the two average spectra corresponding to the first disorder realization must be roughly similar to the true disorder averaged spectra.

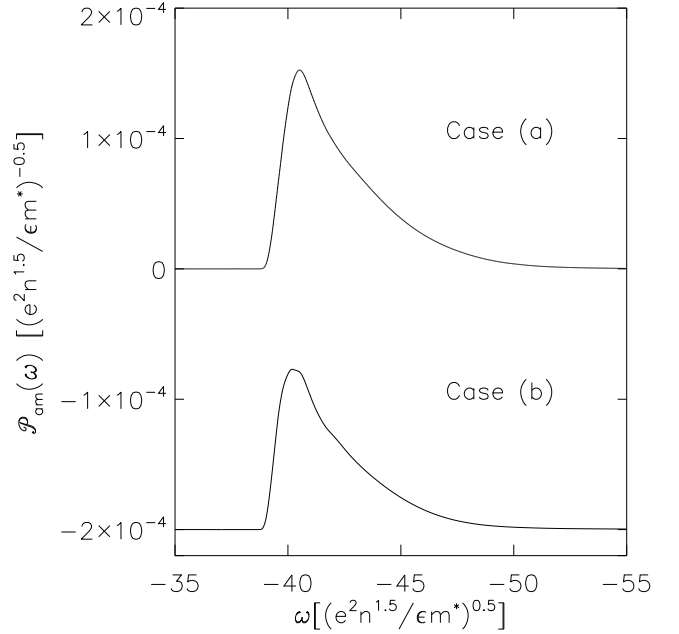


FIG. 8. The figure shows the average spectra corresponding to the disorder realization shown in Fig. 6. Case (a) corresponds to all in-plane electrons being unpinned whereas case (b) corresponds to there being two additional in-plane pinning centers. As expected (see Fig. 7) the average spectra are very wide: roughly three times that observed by Kukushkin *et al.*⁸

IV. CONCLUSION

The line shape of the PL spectra due to electron recombination from a finite and pinned two dimensional Wigner crystal to a hole bound to an acceptor atom, computed using the harmonic approximation and first order time dependent perturbation theory, is similar to that seen in experiment - it has a faster rising as compared to the falling edge. However, the width of the calculated spectra, for recombination events beginning with the perfect lattice configuration of electrons, is only the $\sim 1/3$ of that observed in experiment.⁸ With the initial configuration of electrons being disordered due to charged acceptor atoms corresponding to already recombined electrons, the spectral width is about three times the experimental value. We have speculated that considering lesser disordered configurations and recombination events different from those studied here may result in better agreement with experiment. Since disorder in our model is due only to charged acceptor atoms we speculate that any correlations in their positions (that have been assumed to be zero here) may also reduce the corresponding computed spectral width. Because our perfect crystal and random disorder calculations give results factors of three smaller and larger than the experimental PL width respectively, one could perhaps get *quantitative* agreement with the experimental spectra (we emphasize that our theoretical results are in good qualitative agreement with the experimental PL spectra) by using an adjustable correlated

disorder model, but we feel that, in the absence of any concrete information about the nature of disorder, this is not a particularly meaningful exercise.

V. ACKNOWLEDGMENTS

This work has been supported by the U.S. ONR, the U.S. ARO, the NSF, and the Research Corporation. One of the authors (S. Kodiyalam) thanks Rodney Price, O.W. Greenberg, Lian Zheng, Alpan Raval and Mitrjit Dutta for useful discussions.

APPENDIX A: EWALDS SUMS

The lattice sums appearing in the potential energy terms of Eq. 1 can be obtained as a special case of the following sum for E :

$$E(\vec{r}, \vec{q}, z, p, d) = \sum_{\vec{R}} \frac{e^{i\vec{q} \cdot \vec{R}}}{|\vec{r} + z\hat{e}_z + \vec{R}|^p} - \frac{\theta(\vec{r} + z\hat{e}_z = 0)}{|\vec{r} + z\hat{e}_z|^p} - \frac{\theta(p \leq d, \vec{q} = 0)}{A} \int \frac{d^d r' e^{i\vec{q} \cdot \vec{r}'}}{|\vec{r} + z\hat{e}_z + \vec{r}'|^p}, \quad (A1)$$

with $\vec{R} = \sum_{i=1}^d m_i \vec{a}_i$, $m_i \in \text{integers}$, $\vec{a}_i \cdot \hat{e}_z = 0 \forall i$.

In the above formula \vec{a}_i are the primitive lattice vectors of the d dimensional direct space lattice, and A is the unit cell volume. \vec{r} is assumed to lie *within* the region spanned by the unit cells touching the origin of the direct lattice. Similarly, \vec{q} is assumed to lie *within* the region spanned by the unit cells touching the origin of the reciprocal lattice, the unit cell of which is defined by the vectors \vec{b}_i that are determined by the following:

$$\vec{a}_i \cdot \vec{b}_j = 2\pi\delta_{ij}.$$

The unit vector \hat{e}_z in Eq. A1 does not belong to the space spanned by \vec{a}_i and lies along an additional dimension “perpendicular” to the direct space lattice. p may be any positive real number. The function θ is equal to one if all the conditions in its argument are true and zero otherwise. In the Madelung sum, we are interested in the interaction energy of a particle with all other particles, including its images in other unit cells. This is most conveniently handled by a sum over the Bravais lattice vectors (first term in Eq. A1), but then one must remove the interaction of a particle with itself (second term in Eq. A1). For long range interactions ($p \geq d$), such sums diverge unless an interaction with a neutralizing background is introduced. This is the meaning of the last term in Eq. A1. \tilde{V} that appears in Eq. 1 may now be written as:

$$\tilde{V}(\vec{r}, z) = \frac{e^2}{\epsilon_0} E(\vec{r}, 0, z, 1, 2).$$

Each term of the lattice sum (LS) (the summation in Eq. A1) for E can be written as a sum of a rapidly decreasing function $f_1(\vec{R})$ and another function $f_2(\vec{R})$ that is slowly varying. This division is achieved by multiplying the terms by the following expression for unity in terms of gamma functions:

$$1 = \left[\Gamma \frac{p}{2} \right]^{-1} \left[\Gamma \left(\frac{p}{2}, \epsilon^2 x^2 \right) + \gamma \left(\frac{p}{2}, \epsilon^2 x^2 \right) \right],$$

where

$$x = |\vec{r} + z\hat{e}_z + \vec{R}|, \quad \Gamma(a, b) = \int_b^\infty e^{-t} t^{a-1} dt, \\ \Gamma_a = \Gamma(a, 0), \quad \gamma(a, b) = \Gamma_a - \Gamma(a, b),$$

and ϵ is a suitably chosen (inverse length scale) convergence parameter the choice of which is explained later in this section. Hence the functions f_1 and f_2 may be identified as:

$$f_1(\vec{R}) = \Gamma \frac{p}{2} x^{-p} e^{i\vec{q} \cdot \vec{R}} \Gamma \left(\frac{p}{2}, \epsilon^2 x^2 \right), \quad (A2)$$

$$f_2(\vec{R}) = \Gamma \frac{p}{2} x^{-p} e^{i\vec{q} \cdot \vec{R}} \gamma \left(\frac{p}{2}, \epsilon^2 x^2 \right),$$

with the LS given by

$$LS = \sum_{\vec{R}} f_1(\vec{R}) + \sum_{\vec{R}} f_2(\vec{R}). \quad (A3)$$

Due to the functional form of the gamma function $\Gamma(a, b)$, the terms of the first summation in Eq. A3 die off rapidly with increasing $\epsilon|\vec{R}|$ i.e. for $\epsilon|\vec{R}| \gg 1$,

$$|f_1(\vec{R})| \sim \Gamma \frac{p}{2} \epsilon^p (\epsilon|\vec{R}|)^{-2} e^{-(\epsilon|\vec{R}|)^2}. \quad (A4)$$

Therefore this summation is carried out directly over $\{\vec{R}\}$ (beginning with $\vec{R} = 0$) until the estimated *relative* error due to the neglected terms is smaller than a chosen value.

Due to the functional form of the gamma function $\gamma(a, b)$, the terms of the second summation in Eq. A3 vary slowly with increasing $\epsilon|\vec{R}|$. Therefore their summation is better performed using the following identity that transforms the summation over $\{\vec{R}\}$ of f_2 to a summation over reciprocal lattice vectors ($\{\vec{G}\}$) of the Fourier transform of f_2 (\tilde{f}_2):

$$\sum_{\vec{R}} f_2(\vec{R}) = \int f_2(\vec{r}') \delta_p(\vec{r}') d^d r', \quad \delta_p(\vec{r}') = \sum_{\vec{R}} \delta(\vec{r}' - \vec{R}) \\ \Rightarrow \sum_{\vec{R}} f_2(\vec{R}) = \frac{1}{(2\pi)^d} \int \tilde{f}_2(\vec{k}) \tilde{\delta}_p(-\vec{k}) d^d k,$$

$$\text{where } \tilde{f}_2(\vec{k}) = \int f_2(\vec{r}') e^{i\vec{k} \cdot \vec{r}'} d^d r' ,$$

$$\tilde{\delta}_p(\vec{k}) = \int \delta_p(\vec{r}') e^{i\vec{k} \cdot \vec{r}'} d^d r' = \frac{(2\pi)^d}{A} \sum_{\vec{G}} \delta(k - \vec{G}) ,$$

with $\vec{G} = \sum_{i=1}^d m_i \vec{b}_i$, $m_i \in \text{integers}$, so that

$$\sum_{\vec{R}} f_2(\vec{R}) = \frac{1}{A} \sum_{\vec{G}} \tilde{f}_2(-\vec{G}) .$$

$\tilde{f}_2(\vec{k})$ is computed to be:

$$\tilde{f}_2(\vec{k}) = \frac{\Gamma_{\frac{p}{2}}^{-1} \epsilon^p}{(\epsilon/\sqrt{\pi})^d} e^{-i(\vec{k} + \vec{q}) \cdot \vec{r}} \Upsilon\left(\frac{d-p}{2}, \left|\frac{\vec{k} + \vec{q}}{2\epsilon}\right|^2, \epsilon^2 z^2\right) ,$$

where $\Upsilon(a, b, c) = \int_1^\infty e^{-(\frac{c}{t} + bt)} t^{a-1} dt$, and hence

$$\sum_{\vec{R}} f_2(\vec{R}) = \sum_{\vec{G}} \frac{\Gamma_{\frac{p}{2}}^{-1} \epsilon^p}{A(\epsilon/\sqrt{\pi})^d} \times$$

$$e^{i(\vec{G} - \vec{q}) \cdot \vec{r}} \Upsilon\left(\frac{d-p}{2}, \left(\frac{y}{2\epsilon}\right)^2, \epsilon^2 z^2\right) , \quad (\text{A5})$$

with $y = |\vec{G} - \vec{q}|$.

It must be noted that $\Upsilon(a, b, c) \leq \Upsilon(a, b, 0) = b^{-a} \Gamma(a, b)$. Therefore, again due to the functional form of the gamma function $\Gamma(a, b)$, the terms in the second summation of Eq. A5 die off rapidly with increasing $\frac{|\vec{G}|}{2\epsilon}$ i.e. for $\frac{|\vec{G}|}{2\epsilon} \gg 1$

$$\frac{|\tilde{f}_2(-\vec{G})|}{A} \lesssim \frac{\Gamma_{\frac{p}{2}}^{-1} \epsilon^p}{A(\epsilon/\sqrt{\pi})^d} \left(\frac{|\vec{G}|}{2\epsilon}\right)^{-2} e^{-\left(\frac{|\vec{G}|}{2\epsilon}\right)^2} . \quad (\text{A6})$$

Therefore the second summation in Eq. A3 is transformed using A5 and is carried out over $\{\vec{G}\}$ (beginning with $\vec{G} = 0$) until the estimated *relative* error due to the neglected terms is smaller than a chosen value.

E can now be written (using Eqs. A1, A2, A3 and A5) as:

$$E(\vec{r}, \vec{q}, z, p, d) =$$

$$\Gamma_{\frac{p}{2}}^{-1} \epsilon^p \sum_{\vec{R}} \frac{e^{i\vec{q} \cdot \vec{R}} \Gamma\left(\frac{p}{2}, \epsilon^2 |\vec{r} + z\hat{e}_z + \vec{R}|^2\right)}{(\epsilon |\vec{r} + z\hat{e}_z + \vec{R}|)^p} - \frac{\theta(\vec{r} + z\hat{e}_z = 0)}{|\vec{r} + z\hat{e}_z|^p}$$

$$+ \frac{\Gamma_{\frac{p}{2}}^{-1} \epsilon^p}{A(\epsilon/\sqrt{\pi})^d} \sum_{\vec{G}} e^{i(\vec{G} - \vec{q}) \cdot \vec{r}} \Upsilon\left(\frac{d-p}{2}, \left(\frac{|\vec{G} - \vec{q}|}{2\epsilon}\right)^2, \epsilon^2 z^2\right)$$

$$- \frac{\theta(p \leq d, \vec{q} = 0)}{A} \int \frac{d^d r' e^{i\vec{q} \cdot \vec{r}'}}{|\vec{r} + z\hat{e}_z + \vec{r}'|^p} .$$

It may be rewritten, separating the possibly singular terms (corresponding to $\vec{R} = 0$ and $\vec{G} = 0$) and evaluating them as appropriate limiting cases (of $\vec{r} + z\hat{e}_z \rightarrow 0$ and $\vec{q} \rightarrow 0$ respectively) as:

$$E(\vec{r}, \vec{q}, z, p, d) = \quad (\text{A7})$$

$$\Gamma_{\frac{p}{2}}^{-1} \epsilon^p \left[x + \sum_{\vec{R} \neq 0} \frac{e^{i\vec{q} \cdot \vec{R}} \Gamma\left(\frac{p}{2}, \epsilon^2 |\vec{r} + z\hat{e}_z + \vec{R}|^2\right)}{(\epsilon |\vec{r} + z\hat{e}_z + \vec{R}|)^p} \right]$$

$$+ \frac{\Gamma_{\frac{p}{2}}^{-1} \epsilon^p}{A(\epsilon/\sqrt{\pi})^d} \left[y e^{-i\vec{q} \cdot \vec{r}} + \sum_{\vec{G} \neq 0} e^{i(\vec{G} - \vec{q}) \cdot \vec{r}} \Upsilon\left(\frac{d-p}{2}, \left(\frac{|\vec{G} - \vec{q}|}{2\epsilon}\right)^2, \epsilon^2 z^2\right) \right] ,$$

with

$$x = \begin{cases} \frac{\Gamma\left(\frac{p}{2}, \epsilon^2, |\vec{r} + z\hat{e}_z|^2\right)}{\epsilon |\vec{r} + z\hat{e}_z|^p} & \text{if } \vec{r} + z\hat{e}_z \neq 0 \\ -\frac{2}{p} & \text{if } \vec{r} + z\hat{e}_z = 0 \end{cases}$$

$$y = \begin{cases} \Upsilon\left(\frac{d-p}{2}, \left(\frac{|\vec{q}|}{2\epsilon}\right)^2, \epsilon^2 z^2\right) & \text{if } p > d \text{ or } \vec{q} \neq 0 \\ -\Upsilon\left(\frac{p-d}{2}, \epsilon^2 z^2, 0\right) & \text{if } p \leq d \text{ and } \vec{q} = 0 . \end{cases}$$

Equation A7 can be used to evaluate E for all values of its arguments. First and second derivatives of E (with respect to \vec{r}) that are needed to compute the forces and the dynamical matrix are also obtained by performing the requisite operations on the above expression. For *equally rapid* convergence of the two summations in this equation, ϵ must be given by:

$$\epsilon = \frac{\sqrt{\pi}}{A^{1/d}} . \quad (\text{A8})$$

With this choice of ϵ , the magnitudes of the largest term neglected ($|\delta T|$), if N of the largest terms are included in each of the two summations, become equal - and may be estimated (using Eqs. A4 and A6) to be:

$$|\delta T| = \Gamma_{\frac{p}{2}}^{-1} \left(\frac{\sqrt{\pi}}{A^{1/d}} \right)^p \times \xi^{-2} e^{-\xi^2} , \quad \xi = \left(\Gamma \frac{d}{2} + 1 N \right)^{1/d} .$$

From previous work,¹⁷ $\Upsilon(a, b, c)$ can be written in terms of Gamma functions for a being any odd multiple of $\frac{1}{2}$ (and $b \neq 0$) using:

$$\Upsilon(a, b, c) = \frac{1}{b} \left[e^{-(b+c)} + a \Upsilon(a-1, b, c) + c \Upsilon(a-2, b, c) \right] ,$$

$$\Upsilon\left(\frac{1}{2}, b, c\right) = \frac{1}{2\sqrt{b}} [\alpha + \beta] , \quad \Upsilon\left(-\frac{1}{2}, b, c\right) = \frac{1}{2\sqrt{c}} [\alpha - \beta] ,$$

with

$$\alpha = e^{-2\sqrt{bc}} \left(\Gamma_{\frac{1}{2}} - [\theta(b \geq c) - \theta(b \leq c)] \gamma\left(\frac{1}{2}, |\sqrt{b} - \sqrt{c}|\right) \right),$$

$$\beta = e^{2\sqrt{bc}} \Gamma\left(\frac{1}{2}, \sqrt{b} + \sqrt{c}\right).$$

Finally, an accurate evaluation of Gamma functions (*relative error* $\lesssim 10^{-14}$) is done using the ideas outlined by C. Lanczos.^{23,24}

APPENDIX B: NORMAL MODES OF A GENERAL HARMONIC HAMILTONIAN

This section shows the procedure for transforming a harmonically approximated Hamiltonian of the form

$$\mathcal{H}^h = \epsilon^m + \frac{1}{2m^*} [\Phi^T \Pi^T] \begin{bmatrix} m^* \mathbf{D} + \mathbf{B}^T \mathbf{B} & -\mathbf{B}^T \\ -\mathbf{B} & \mathbf{I} \end{bmatrix} \begin{bmatrix} \Phi \\ \Pi \end{bmatrix}$$

into a summation over uncoupled (normal) modes by a linear canonical transformation of the phase space variables $[\Phi^T \Pi^T]$ (Eqs. 4 and 5). The only requirement for this procedure to apply is that \mathbf{D} be a symmetric positive-definite matrix. This is the case here since \mathbf{D} is the dynamical matrix corresponding to a *stable* equilibrium. (All matrices that appear in this section are real.) The transformation is carried out in three steps which together constitute a canonical transformation. This is verified by simultaneously determining the equations of motion for the transformed variables and showing that they may be derived from the Hamiltonian in the same variables. The equations of motion in the current variables read as:

$$\begin{bmatrix} \dot{\Phi} \\ \dot{\Pi} \end{bmatrix} = \frac{1}{m^*} \begin{bmatrix} -\mathbf{B} & \mathbf{I} \\ -m^* \mathbf{D} - \mathbf{B}^T \mathbf{B} & \mathbf{B}^T \end{bmatrix} \begin{bmatrix} \Phi \\ \Pi \end{bmatrix}.$$

The procedure is similar to the standard technique,²⁵ but has to be extended to a multiparticle generalization.

The first of the three steps in the transformation is in itself a canonical transformation that diagonalizes the dynamical matrix \mathbf{D} . This is accomplished by an orthogonal matrix \mathbf{N} (*i.e.* $\mathbf{N}^T = \mathbf{N}^{-1}$) the existence of which follows from the real symmetric structure of \mathbf{D} . Since the eigenvalues of \mathbf{D} are all positive (as it is a positive definite matrix) the diagonalized result may be written as: $m^* \mathbf{D}_\omega^2 = \mathbf{N}^T \mathbf{D} \mathbf{N}$ where \mathbf{D}_ω is a diagonal matrix with positive elements of the dimension of frequency. The transformed variables may therefore be written as:

$$\begin{bmatrix} \Phi_1 \\ \Pi_1 \end{bmatrix} = \begin{bmatrix} (m^* \mathbf{D}_\omega)^{1/2} \mathbf{N}^T & \mathbf{0} \\ \mathbf{0} & (m^* \mathbf{D}_\omega)^{-1/2} \mathbf{N}^T \end{bmatrix} \begin{bmatrix} \Phi \\ \Pi \end{bmatrix}, \quad (\text{B1})$$

in terms of which the Hamiltonian and the equations of motion read:

$$\mathcal{H}^h = \epsilon^m + \frac{1}{2} [\Phi_1^T \Pi_1^T] \begin{bmatrix} \mathbf{D}_\omega + \mathbf{B}_\omega^T \mathbf{D}_\omega^{-1} \mathbf{B}_\omega & -\mathbf{B}_\omega^T \\ -\mathbf{B}_\omega & \mathbf{D}_\omega \end{bmatrix} \begin{bmatrix} \Phi_1 \\ \Pi_1 \end{bmatrix},$$

$$\begin{bmatrix} \dot{\Phi}_1 \\ \dot{\Pi}_1 \end{bmatrix} = \begin{bmatrix} -\mathbf{B}_\omega & \mathbf{D}_\omega \\ -\mathbf{D}_\omega - \mathbf{B}_\omega^T \mathbf{D}_\omega^{-1} \mathbf{B}_\omega & \mathbf{B}_\omega^T \end{bmatrix} \begin{bmatrix} \Phi_1 \\ \Pi_1 \end{bmatrix},$$

where \mathbf{B}_ω is the transformed \mathbf{B} matrix that also has the dimensions of frequency and is given by: $m^* \mathbf{B}_\omega = \mathbf{D}_\omega^{-1/2} \mathbf{N}^T \mathbf{B} \mathbf{N} \mathbf{D}_\omega^{1/2}$. It may be seen that if $\mathbf{B} = \mathbf{0}$ ($\Rightarrow \mathbf{B}_\omega = \mathbf{0}$) then Eq. B1 would suffice to diagonalize \mathcal{H}^h into the required form.

The next transformation trivially diagonalizes the Hamiltonian. However, as the equations of motion in the new variables do not follow from the Hamiltonian in the same variables, it is not a canonical transformation. The transformation is given by:

$$\begin{bmatrix} \Phi_2 \\ \Pi_2 \end{bmatrix} = \begin{bmatrix} \mathbf{D}_\omega^{1/2} & \mathbf{0} \\ -\mathbf{D}_\omega^{-1/2} \mathbf{B}_\omega & \mathbf{D}_\omega^{1/2} \end{bmatrix} \begin{bmatrix} \Phi_1 \\ \Pi_1 \end{bmatrix}. \quad (\text{B2})$$

In terms of the new variables the Hamiltonian and the equations of motion now read as:

$$\begin{aligned} \mathcal{H}^h &= \epsilon^m + \frac{1}{2} [\Phi_2^T \Pi_2^T] \begin{bmatrix} \mathbf{I} & \mathbf{0} \\ \mathbf{0} & \mathbf{I} \end{bmatrix} \begin{bmatrix} \Phi_2 \\ \Pi_2 \end{bmatrix}, \\ \begin{bmatrix} \dot{\Phi}_2 \\ \dot{\Pi}_2 \end{bmatrix} &= \begin{bmatrix} \mathbf{0} & \mathbf{D}_\omega \\ -\mathbf{D}_\omega & \tilde{\mathbf{B}}_\omega^T - \tilde{\mathbf{B}}_\omega \end{bmatrix} \begin{bmatrix} \Phi_2 \\ \Pi_2 \end{bmatrix} \\ &= \mathbf{Q} \begin{bmatrix} \Phi_2 \\ \Pi_2 \end{bmatrix}, \end{aligned}$$

where $\tilde{\mathbf{B}}_\omega = \mathbf{D}_\omega^{-1/2} \mathbf{B}_\omega \mathbf{D}_\omega^{1/2}$.

The final transformation, which together with the previous one results in a canonical transformation, involves the “block off-diagonalization” of the matrix \mathbf{Q} by an orthogonal matrix \mathbf{M} (*i.e.* $\mathbf{M}^T = \mathbf{M}^{-1}$) the existence of which follows from the real antisymmetric structure of \mathbf{Q} . It must be noted that \mathbf{Q} is an even-dimensional matrix ($2N_f \times 2N_f$) which may be shown to be non-singular since all the diagonal elements of \mathbf{D}_ω are non-zero. \mathbf{M} is constructed using the eigenvectors of another *symmetric* matrix $\tilde{\mathbf{Q}}$:

$$\tilde{\mathbf{Q}} = \begin{bmatrix} \mathbf{0} & \mathbf{Q} \\ -\mathbf{Q} & \mathbf{0} \end{bmatrix}.$$

It can be shown that the eigenvalues of $\tilde{\mathbf{Q}}$ are necessarily non-zero (due to \mathbf{Q} being nonsingular), degenerate by an even number and that corresponding to every eigenvalue there is another with equal magnitude and opposite sign. This can be seen from the construction of the eigenvectors: if there is an eigenvector of the

form $[\mathbf{v}_1^T, \mathbf{v}_2^T]^T$ with eigenvalue ω_1 (\mathbf{v}_1 and \mathbf{v}_2 are column vectors with $2N_f$ components), then the vectors $[\mathbf{v}_2^T, -\mathbf{v}_1^T]^T$, $[\mathbf{v}_2^T, \mathbf{v}_1^T]^T$ and $[-\mathbf{v}_1^T, -\mathbf{v}_2^T]^T$ are also eigenvectors with eigenvalues ω_1 , $-\omega_1$ and $-\omega_1$. It may be shown that the four vectors are mutually orthogonal and hence linearly independent. From the mutual orthogonality of all eigenvectors of \mathbf{Q} constructed in the above fashion (for eigenvalues that are more than two fold degenerate, the corresponding eigenvectors may need an explicit orthogonalization procedure) it can be shown that the vectors \mathbf{v}_1^i , \mathbf{v}_2^i ($i = 1$ to N_f) are mutually orthogonal. They are chosen from the set of eigenvectors of \mathbf{Q} that have $\omega_i > 0$ and are explicitly normalized. The matrix \mathbf{M} is then constructed:

$$\mathbf{M} = [\mathbf{v}_1^1, \mathbf{v}_1^2, \dots, \mathbf{v}_1^{N_f}, \mathbf{v}_2^1, \mathbf{v}_2^2, \dots, \mathbf{v}_2^{N_f}] .$$

It may be verified that \mathbf{M} is orthogonal and that it “block off-diagonalizes” \mathbf{Q} :

$$\mathbf{M}^T \mathbf{Q} \mathbf{M} = \begin{bmatrix} \mathbf{0} & \boldsymbol{\Omega} \\ -\boldsymbol{\Omega} & \mathbf{0} \end{bmatrix} ,$$

where $\boldsymbol{\Omega}$ is a diagonal matrix with the diagonal elements being the (positive) phonon frequencies ω_i . The final transformation is given by:

$$\begin{bmatrix} \boldsymbol{\Psi} \\ \boldsymbol{\Xi} \end{bmatrix} = \begin{bmatrix} \boldsymbol{\Omega}^{-1/2} & \mathbf{0} \\ \mathbf{0} & \boldsymbol{\Omega}^{-1/2} \end{bmatrix} [\mathbf{M}^T] \begin{bmatrix} \boldsymbol{\Phi}_2 \\ \boldsymbol{\Pi}_2 \end{bmatrix} . \quad (\text{B3})$$

In terms of the variables $\boldsymbol{\Psi}$ and $\boldsymbol{\Xi}$ the the Hamiltonian and the equations of motion read:

$$\begin{aligned} \mathcal{H}^h &= \epsilon^m + \frac{1}{2} [\boldsymbol{\Psi}^T \boldsymbol{\Xi}^T] \begin{bmatrix} \boldsymbol{\Omega} & \mathbf{0} \\ \mathbf{0} & \boldsymbol{\Omega} \end{bmatrix} \begin{bmatrix} \boldsymbol{\Psi} \\ \boldsymbol{\Xi} \end{bmatrix} , \\ \begin{bmatrix} \dot{\boldsymbol{\Psi}} \\ \dot{\boldsymbol{\Xi}} \end{bmatrix} &= \begin{bmatrix} \mathbf{0} & \boldsymbol{\Omega} \\ -\boldsymbol{\Omega} & \mathbf{0} \end{bmatrix} \begin{bmatrix} \boldsymbol{\Psi} \\ \boldsymbol{\Xi} \end{bmatrix} . \end{aligned}$$

As the equations of motion for $\boldsymbol{\Psi}$ and $\boldsymbol{\Xi}$ follow from the Hamiltonian in the same variables, the combined transformation \mathbf{C} represented by Eqs. B1, B2 and B3 must be canonical. In other words the transformation \mathbf{C} given by:

$$\begin{aligned} \mathbf{C} &= \begin{bmatrix} \boldsymbol{\Omega}^{-1/2} & \mathbf{0} \\ \mathbf{0} & \boldsymbol{\Omega}^{-1/2} \end{bmatrix} [\mathbf{M}^T] \begin{bmatrix} \mathbf{D}_\omega^{1/2} & \mathbf{0} \\ -\mathbf{D}_\omega^{-1/2} \mathbf{B}_\omega & \mathbf{D}_\omega^{1/2} \end{bmatrix} \\ &\times \begin{bmatrix} (m^* \mathbf{D}_\omega)^{1/2} \mathbf{N}^T & \mathbf{0} \\ \mathbf{0} & (m^* \mathbf{D}_\omega)^{-1/2} \mathbf{N}^T \end{bmatrix} , \end{aligned}$$

may be verified to be canonical, *i.e.* it satisfies:

$$\mathbf{C}^T \boldsymbol{\Sigma} \mathbf{C} = \boldsymbol{\Sigma} , \quad \boldsymbol{\Sigma} = \begin{bmatrix} \mathbf{0} & \mathbf{I} \\ -\mathbf{I} & \mathbf{0} \end{bmatrix} .$$

\mathbf{C} therefore transforms the Hamiltonian into uncoupled normal modes as required (Eqs. 4 and 5).

APPENDIX C: PHOTOLUMINESCENCE FORMULA FROM TIME DEPENDENT PERTURBATION THEORY

In this section we postulate a time independent Hamiltonian \mathcal{H}^a which, on the application of first-order time dependent perturbation theory, yields the PL formula used (Eqs. 16 and 11). (In this section all bold faced vectors have three components (x , y and z) whereas others have only two (x and y): $\vec{\mathbf{v}} = (\vec{v}, v_z)$.)

The Hamiltonian \mathcal{H}^a may be assumed to be an approximation to another Hamiltonian \mathcal{H} that has been postulated previously²⁶ to include the (first quantized) degrees of freedom for (spinless) electrons (corresponding here to unpinned electrons, N_f in number) with the electromagnetic fields considered to be the sum of two fields - internal fields that are due to the electronic degrees of freedom and external fields (here the uniform magnetic field in the z direction and the electric fields due to pinned electrons and any required confinement potentials) that are independently specified. The internal fields are considered dynamical - their energy therefore included in \mathcal{H} . These fields are represented through a four vector potential $(\vec{\mathbf{A}}^p, \phi^p)$ in the Coulomb gauge: $\vec{\nabla} \cdot \vec{\mathbf{A}}^p = 0$. It may be seen that in this gauge $\vec{\mathbf{A}}^p$ is dynamical (and therefore quantized) whereas ϕ^p is not - it is completely determined by the electronic degrees of freedom as the total Coulomb potential. Its contribution to the field energy results is the Coulomb interaction between the electrons. The external fields are considered non-dynamical and therefore do not contribute to the field energy. They are specified through another four vector potential $(\vec{\mathbf{A}}, \phi)$ that is a function of the electronic degrees of freedom and whose gauge is chosen independently. Both the types of fields are minimally coupled to all the electronic degrees of freedom. This gives:

$$\mathcal{H} = \mathcal{H}_0 + \mathcal{H}_I , \quad \mathcal{H}_0 = \mathcal{H}_0^e + \mathcal{H}_0^p , \quad (\text{C1})$$

where

$$\begin{aligned} \mathcal{H}_0^e &= \sum_k \left[\frac{1}{2m} \left[\vec{\mathbf{p}}_k - \frac{e}{c} \vec{\mathbf{A}}(\vec{\mathbf{r}}_k) \right]^2 + e\phi(\vec{\mathbf{r}}_k) + \sum_{l>k} \frac{e^2}{|\vec{\mathbf{r}}_k - \vec{\mathbf{r}}_l|} \right] , \\ \mathcal{H}_0^p &= \sum_{\vec{\mathbf{k}}, r} \hbar\omega_{\vec{\mathbf{k}}} a_{\vec{\mathbf{k}}, r}^\dagger a_{\vec{\mathbf{k}}, r} , \\ \mathcal{H}_I &= \sum_k \left[\frac{-e}{mc} \vec{\mathbf{A}}^p(\vec{\mathbf{r}}_k) \cdot \left[\vec{\mathbf{p}}_k - \frac{e}{c} \vec{\mathbf{A}}(\vec{\mathbf{r}}_k) \right] + \frac{e^2}{2mc^2} \left[\vec{\mathbf{A}}^p(\vec{\mathbf{r}}_k) \right]^2 \right] , \end{aligned}$$

with

$$\begin{aligned} \vec{\mathbf{A}}^p(\vec{\mathbf{r}}) &= \sqrt{\frac{\hbar c^2}{2V\omega_{\vec{\mathbf{k}}}}} \sum_{\vec{\mathbf{k}}, r} \hat{\epsilon}_{\vec{\mathbf{k}}, r} \left[a_{\vec{\mathbf{k}}, r} e^{i\vec{\mathbf{k}} \cdot \vec{\mathbf{r}}} + a_{\vec{\mathbf{k}}, r}^\dagger e^{-i\vec{\mathbf{k}} \cdot \vec{\mathbf{r}}} \right] \\ \omega_{\vec{\mathbf{k}}} &= c|\vec{\mathbf{k}}| ; \hat{\epsilon}_{\vec{\mathbf{k}}, r} \cdot \hat{\epsilon}_{\vec{\mathbf{k}}, s} = \delta_{r,s} ; \hat{\epsilon}_{\vec{\mathbf{k}}, r} \cdot \vec{\mathbf{k}} = 0 ; r, s = 1, 2 . \\ \{a_{\vec{\mathbf{k}}, r}, a_{\vec{\mathbf{k}}', s}^\dagger\} &= \delta_{\vec{\mathbf{k}}, \vec{\mathbf{k}}'} \delta_{r,s} \quad \{a_{\vec{\mathbf{k}}, r}, a_{\vec{\mathbf{k}}', s}\} = 0 . \end{aligned}$$

In the above the index k varies from 1 to N_f , \vec{k} takes on all values such that $\vec{A}^p(\vec{r})$ is periodic over cube-like volumes V and curly brackets imply commutation.

We now go over to our case of a two dimensional electron system by first identifying m to be the effective mass m^* and introducing the dielectric constant ϵ_0 into the electron-electron interactions. The interactions are also modified to take into account the periodic boundary conditions used (in section II). \vec{A} is chosen to correspond to the external magnetic field in the z direction *i.e.* $\vec{A}(\vec{r}) = (\vec{A}(\vec{r}), 0)$. We then introduce approximations/assumptions into \mathcal{H}_0^e that result in the loss of the indistinguishability of electrons. The first of these involves the external potential ϕ . It is assumed that $e\phi(\vec{r}) = V_c(z) + V_p(\vec{r})$ where $V_p(\vec{r})$ is due to the pinned electrons and $V_c(z)$ is assumed to confine the electrons at particular values of z . We then assume that $V_c(z)$ takes on two different functional forms - the first allowing for only one state in which the electron is confined to the x - y plane and the second allowing for an additional state in which the electron is confined a distance z_0 away from the x - y plane (corresponding to the z position of the holes bound to the acceptor atoms). The first functional form is assumed to apply to all the electrons except the recombining electron (index $k = c$) for which the second functional form is assumed to apply. This distinguishes the the recombining electron from the other electrons. We then make the harmonic approximation (as described in section II) which distinguishes all the electrons and results in the construction of the two Hamiltonians \mathcal{H}_i^h and \mathcal{H}_f^h corresponding respectively to the states in which the z degree of freedom of the recombining electron is confined to the x - y plane or at a distance z_0 from this plane. As this approximation is made only for the x - y degrees of freedom, the z dependence of $V_p(\vec{r})$ and the electron-electron interactions enters only as parameters of the harmonically approximated Hamiltonians $\mathcal{H}_{i,f}^h$. All the above approximations/assumptions are encoded in the following declaration for the approximated form ($\mathcal{H}_0^{e,a}$) of the Hamiltonian \mathcal{H}_0^e in which the electronic z degrees of freedom are decoupled from the x - y degrees of freedom. With the operators written in the space of x - y electronic degrees of freedom $\otimes z$ electronic degrees of freedom, $\mathcal{H}_0^{e,a}$ may be written as:

$$\begin{aligned}\mathcal{H}_0^{e,a} &= \mathcal{H}_i^h \otimes P_0 + \mathcal{H}_f^h \otimes P_{z_0} + I \otimes \mathcal{H}_z, \\ \mathcal{H}_z &= H'(z_c, p_{z_c}) + \sum_{k \neq c} H(z_k, p_{z_k}),\end{aligned}$$

where, as mentioned previously, $H(z, p_z)$ admits only one state localized around $z = 0$ whereas $H'(z, p_z)$ admits an additional state localized around $z = z_0$. P_0 (P_1) is the projection operator onto the multiparticle eigenfunction for the z degrees of freedom of the electrons $|\psi_0^z\rangle$ ($|\psi_{z_0}^z\rangle$) that has the recombining electron localized around $z = 0$ ($z = z_0$) - with the corresponding eigenvalue with respect to \mathcal{H}_z being 0 ($-E^b$). E^b can be considered to be

the electron-hole binding energy that is an undetermined parameter in this theory.

The approximate form of \mathcal{H}_0 is now written as:

$$\mathcal{H}_0^a = \mathcal{H}_0^{e,a} + \mathcal{H}_0^p, \quad (C2)$$

which may be seen to have the following eigenfunctions that constitute an orthonormal basis:

$$\{|\Psi_I\rangle = |\psi_i\rangle \otimes |\psi_0^z\rangle \otimes |\psi^p\rangle, |\Psi_F\rangle = |\psi_f\rangle \otimes |\psi_{z_0}^z\rangle \otimes |\psi^p\rangle\},$$

where (as defined in section II) $|\psi_i\rangle$ ($|\psi_f\rangle$) is an eigenstate of \mathcal{H}_i^h (\mathcal{H}_f^h) with eigenvalue E_i (E_f) and $|\psi^p\rangle$ is an eigenstate of \mathcal{H}_0^p that has a definite number of photons $n_{\vec{k},r}$ in each mode (\vec{k}, r) (\Rightarrow eigenvalue $E^p = \sum_{\vec{k},r} \hbar\omega_{\vec{k}} n_{\vec{k},r}$). Therefore:

$$\begin{aligned}\mathcal{H}_0^a |\Psi_I\rangle &= E_I |\Psi_I\rangle, \quad E_I = E_i + E^p, \\ \mathcal{H}_0^a |\Psi_F\rangle &= E_F |\Psi_F\rangle, \quad E_F = E_f - E^b + E^p.\end{aligned}$$

We now approximate \mathcal{H}_I (Eq. C1) using: $\mathcal{A}^p(\vec{r}_k) \approx \mathcal{A}^p(\vec{r}_k^0)$ where \vec{r}_k^0 is the average of the classical equilibrium positions of electron k before and after the recombination process. This is the dipole approximation that may be justified using input from the experiment⁸ that we are attempting to model here - the PL peak is at a wavelength $\approx 8230\text{\AA}$ (with the width being very small: $\approx 20\text{\AA}$) which would be much larger than the spread in the \mathbf{r}_k as computed using $|\Psi_{I,F}\rangle$ or the change in the classical equilibrium value of \mathbf{r}_k due to the recombination process. Therefore:

$$\begin{aligned}\mathcal{H}_I^a &= \frac{-e}{m^* c} \sum_k \left[\vec{A}^p(\vec{r}_k^0) \cdot \left[\vec{p}_k - \frac{e}{c} \vec{A}(\vec{r}_k) \right] + A_z^p(\vec{r}_k^0) p_{z_k} \right] \\ &\quad + \frac{e^2}{2m^* c^2} \sum_k \left[\vec{A}^p(\vec{r}_k^0) \right]^2\end{aligned} \quad (C3)$$

where, in the first summation, the x - y components has been separated from the z component of the vectors.

We now construct the approximate form of \mathcal{H} (Eq. C1) using Eqs. C2 and C3:

$$\mathcal{H}^a = \mathcal{H}_0^a + \mathcal{H}_I^a \quad (C4)$$

\mathcal{H}^a is the Hamiltonian in this study. First order time dependent perturbation theory (Fermi's golden rule) may now be applied to compute the intensity of photons emitted $I_+(\omega)$ (or absorbed $I_-(\omega)$). The computation is now analogous to calculations of radiative transitions in atoms - here all the N_f electrons constitute the "atom". The initial states are declared to be of the form $|\Psi_I\rangle$ (recombining electron localized around $z = 0$) and the final states of the form $|\Psi_F\rangle$ (recombining electron localized around $z = z_0$). For emission calculations it is assumed that the initial state $|\Psi_I\rangle_+$ has no photons and the corresponding final state $|\Psi_F\rangle_+$ has a single photon with a frequency between ω and $\omega + d\omega$ whereas for absorption calculations the opposite is assumed. Initial states

$|\Psi_I\rangle_{\pm}$ that satisfy the requisite constraints on the photon numbers are further assumed to be thermally distributed. The application of the Fermi's golden rule now gives:

$$I_{\pm}(\omega)d\omega = \frac{2\pi}{\hbar} \frac{\sum_I e^{-\beta E_I} \sum_F |\pm \langle \Psi_F | \mathcal{H}_I^a | \Psi_I \rangle_{\pm}|^2 \delta(E_I - E_F)}{\sum_I e^{-\beta E_I}}$$

It may be seen that only one term ($-eA_z^p(\vec{r}_c^0)p_{z_c}/m^*c$) in Eq. C3, for \mathcal{H}_I^a , can have a non-zero matrix element between the states $|\Psi_I\rangle_{\pm}$ and $|\Psi_F\rangle_{\pm}$ since these differ in the z state of the recombining electron. No other term in Eq. C3 has any dependence on the operators corresponding to the z degree of freedom of the recombining electron (z_c, p_{z_c}). $I_{\pm}(\omega)$ is therefore given by the following expression in which the photon states $|\psi^p\rangle$ do not appear:

$$I_{\pm}(\omega) = C(\omega) \left\langle [\hat{\epsilon}_{\hat{r},1}^z]^2 + [\hat{\epsilon}_{\hat{r},2}^z]^2 \right\rangle_{\Delta\Omega} \Delta\Omega \mathcal{P}(\pm\omega - \hbar^{-1}E^b),$$

$$C(\omega) = \frac{|\omega|}{8\hbar c} \left[\frac{e|\langle \psi_{z_0}^z | p_{z_c} | \psi_0^z \rangle|}{\pi m^* c} \right]^2, \quad (C5)$$

where $\Delta\Omega$ is the solid angle over which photons of momentum $\vec{k} = (\omega/c)\hat{r}$ are detected (\hat{r} being a unit vector), $\langle \rangle_{\Delta\Omega}$ is the average over the solid angle, $\hat{\epsilon}^z$ is the z component of $\hat{\epsilon}$ and \mathcal{P} is given by Eq. 11 (section II). From the above it can be seen that $I_-(\omega) = I_+(-\omega)$. Hence, both emission and absorption intensities can be given by I_+ with the convention that negative ω corresponds to absorption of photons. An important prediction from the above formula is that photons are fully *polarized*. This is most easily seen by noting that the transition involves motion of an electron in the z direction, which can couple only to the electric fields with a \hat{z} component. Since the polarizations of the photons in the equations below C1 may be specified with one polarization in the x - y plane, this photon does not couple to the transition. Thus, the polarization of an emitted photon will be in the $\hat{k} \times [\hat{z} \times \hat{k}]$ direction. Lastly, using again experimental input that the PL peak width is much smaller than the average photon frequency ω_{av} , $C(\omega)$ may be replaced by $C(\omega_{av})$. This gives:

$$I(\omega) = C(\omega_{av}) \langle (\hat{\epsilon}_{\hat{r},1}^z)^2 \rangle_{\Delta\Omega} \Delta\Omega \mathcal{P}(\omega - \hbar^{-1}E^b). \quad (C6)$$

This justifies Eqs. 16 and 11 which have $E^b = 0$. It can now be seen that the calculated peak in $I(\omega)$ can be shifted along the ω axis to agree with the experimentally observed peak position through a suitable choice of E^b .

APPENDIX D: APPROXIMATIONS AND CONVERGENCE CRITERIA

Here we describe approximations to $\mathcal{P}(\omega)$ that provides a cutoff to the integral in Eq. 12 and also discretizes it to a summation.

It must be noted that $\mathcal{P}(\omega)$ is calculated for a finite system and therefore it consists of a series of delta functions as can be seen in Eq. 11. The summations in this equation *do not* go over to integrals as would be the case for an infinite system. Therefore, for $\mathcal{P}(\omega)$ to be a continuous curve even in the case of a finite system, the delta function in Eq. 11 must be replaced by a function with non-zero width. We have chosen this function to be a Gaussian with width Γ_0 , *i.e.*

$$\text{with } g(\Gamma, \omega) = \frac{1}{\sqrt{2\pi\Gamma}} e^{-\frac{\omega^2}{2\Gamma^2}},$$

$$\mathcal{P}_a(\omega) = \frac{\sum_i e^{-\beta E_i} \sum_f |\langle \psi_f | \psi_i \rangle|^2 g(\Gamma_0, \hbar^{-1}(E_i - E_f) - \omega)}{\sum_i e^{-\beta E_i}}.$$

The choice of Γ_0 varies with the cases studied - the corresponding values are specified in section III. It can be shown that the approximated $\mathcal{P}(\omega)$ ($\mathcal{P}_a(\omega)$) can be obtained from $\tilde{\mathcal{P}}(t)$ as given by Eq. 13 using:

$$\mathcal{P}_a(\omega) = \frac{1}{2\pi} \int_{-\infty}^{+\infty} dt e^{-i\omega t} e^{-\frac{\Gamma_0^2 t^2}{2}} \tilde{\mathcal{P}}(t).$$

The integral can therefore be cutoff between the limits $[-T, T]$ such that the error in $\mathcal{P}_a(\omega)$ due to this ($\delta\mathcal{P}_a(\omega)$) is a small fraction (f) of the expected maximum in $\mathcal{P}_a(\omega)$ (peak height). Assuming that $\mathcal{P}_a(\omega)$ consists of a *single* peak that is Gaussian in shape (this is roughly the experimental line shape⁸), the expected peak height in terms of the estimated (upper bound) peak width σ_{est}^u is equal to $\tilde{\mathcal{P}}(t = 0)/\sqrt{2\pi\sigma_{est}^u}$. Further it can be shown that $|\tilde{\mathcal{P}}(t)|$ is maximum at $t = 0$ ($=1$ from Eq. 13). Therefore T is chosen such that:

$$|\delta\mathcal{P}_a(\omega)| \leq \tilde{\mathcal{P}}(0) \times 2 \int_T^{\infty} e^{-\frac{\Gamma_0^2 t^2}{2}} dt \leq \frac{\tilde{\mathcal{P}}(0)f}{\sqrt{2\pi\sigma_{est}^u}}$$

$$\Rightarrow T \mid \Gamma\left(\frac{1}{2}, \frac{\Gamma_0^2 T^2}{2}\right) \leq \frac{f\sqrt{\pi}\Gamma_0}{\sigma_{est}^u} \quad (D1)$$

(The gamma function $\Gamma(a, b)$ has been defined in Appendix A.) f is chosen to be 10^{-4} throughout this study. The choice of σ_{est}^u varies with the cases studied - its values chosen conservatively to be larger than the expected variance of ω in the spectrum being computed. $\mathcal{P}_a(\omega)$ is therefore given by:

$$\mathcal{P}_a(\omega) = \frac{1}{2\pi} \int_{-T}^{+T} dt e^{-i\omega t} e^{-\frac{\Gamma_0^2 t^2}{2}} \tilde{\mathcal{P}}(t),$$

$$\text{with } \omega = n \frac{2\pi}{2T}, \quad n \in \text{integers},$$

where the discretization of ω follows from the finiteness of the time domain integral.

We now present a modification to $\tilde{\mathcal{P}}(t)$ that aids in approximating the above integral to a summation and also justifies the assumption that (the modified) $\mathcal{P}_a(\omega)$ consists of only one peak. As mentioned in the previous section, the parameter λ_f in \mathcal{H}_f is chosen to be large so as to “suppress” the x - y degrees of freedom of the recombining electron into becoming “irrelevant” in \mathcal{H}_f . We have chosen it to be $10^3 e^2 n^{1.5}/\epsilon_0$ throughout this study. This makes *two* normal modes of \mathcal{H}_f^h have very large frequencies. These “ λ modes” may be identified as those whose frequency has the strongest dependence on the value of λ_f . It is found (in systems with $N_f = 9$) that the initial states $|\psi_i\rangle$ *do* have a significant overlap with final states $|\psi_f\rangle$ whose λ modes are excited *i.e.* then final state $|\psi_f\rangle$ has one or more of the λ mode phonons. As a result the $\mathcal{P}_a(\omega)$ consists of peaks that are separated from each other by the λ mode frequencies with only a small fraction of the total area under the first peak closest to $\omega = 0$ (total area = $\tilde{\mathcal{P}}(t = 0) = 1$). All the peaks are centered around points with $\omega < 0$ since the ground state energy of \mathcal{H}_f^h is greater than that of \mathcal{H}_i^h (which is primarily due to the zero point energy of the λ modes in \mathcal{H}_f^h as well as because $\epsilon_f^m > \epsilon_i^m$). In other words, in the absence of an additional term in \mathcal{H}_f^h corresponding to the (negative) binding energy of the electron to the hole all the peaks correspond to absorption rather than emission of photons (see Appendix C). We presume that *only the first peak* is relevant to the experiment *i.e.* we assume that the electron-hole binding energy (which is not determined within our model) is sufficient to shift the peaks such that only the first peak comes into the positive ω domain. This identification is motivated by the assumption that the final states $|\psi_f\rangle$ with no λ mode phonons best represent the “true” state of the recombined electron (with a more realistic Hamiltonian) since, of the different $|\psi_f\rangle$ with varying number of λ mode phonons, it is these states that maximally localize the recombined electron.

Having argued that only the first peak is of interest, the other peaks may be removed from $\mathcal{P}_a(\omega)$ and thereby reduce its width to that of the first peak. This is achieved by exponentially suppressing the irrelevant peaks *i.e.* $\mathcal{P}_a(\omega)$ is modified to $\mathcal{P}_{am}(\omega)$ given by:

$$\mathcal{P}_{am}(\omega) = \left[\sum_i e^{-\beta E_i} \right]^{-1} \sum_i e^{-\beta E_i} \times \sum_f |\langle \psi_f | \psi_i \rangle|^2 e^{-\gamma(n_1^\lambda + n_2^\lambda)} g(\Gamma_0, \hbar^{-1}(E_i - E_f) - \omega),$$

where n_1^λ and n_2^λ are the numbers of the two λ mode phonons in $|\psi_f\rangle$. It can be shown (using arguments similar to those leading to Eqs. 12-15) that its Fourier transform $\tilde{\mathcal{P}}_{am}(t)$ is given by:

$$\tilde{\mathcal{P}}_{am}(t) = e^{-\frac{\Gamma_0^2 t^2}{2}} \left(\text{Tr} \left[e^{-\beta \mathcal{H}_i^h} \right] \right)^{-1} \times e^{\gamma \text{Tr} \left[e^{-i\hbar^{-1} \tilde{\mathcal{H}}_f^h t} e^{i\hbar^{-1} \mathcal{H}_i^h (t + i\hbar\beta)} \right]}, \quad (\text{D2})$$

with

$$\begin{aligned} \tilde{\mathcal{H}}_f^h &= \mathcal{H}_f^h(\Omega_f \rightarrow \Omega_f - i\frac{\mathbf{D}_\gamma}{t}), \\ &= \frac{\hbar}{2} \left[\tilde{\mathbf{a}}_f \tilde{\mathbf{a}}_f^\dagger \right] \left[\tilde{\mathbf{\Omega}}_f \right] \begin{bmatrix} \mathbf{a}_f \\ \mathbf{a}_f^\dagger \end{bmatrix} + \epsilon_f^m, \\ \tilde{\mathbf{\Omega}}_f &= \begin{bmatrix} \mathbf{0} & \Omega_f - i\frac{\mathbf{D}_\gamma}{t} \\ \Omega_f - i\frac{\mathbf{D}_\gamma}{t} & \mathbf{0} \end{bmatrix}, \end{aligned} \quad (\text{D3})$$

where \mathbf{D}_γ is a diagonal matrix with γ corresponding to the two λ modes and zero otherwise. Calculation of the traces appearing in Eq. D2 has been outlined in Appendix E.²⁷ Hence $\mathcal{P}_{am}(\omega)$ given by:

$$\begin{aligned} \mathcal{P}_{am}(\omega) &= \frac{1}{2\pi} \int_{-T}^{+T} dt e^{-i\omega t} \tilde{\mathcal{P}}_{am}(t), \\ \omega &= \frac{n\pi}{T}, \end{aligned} \quad (\text{D4})$$

where the cutoff T continues to be given by Eq. D1. The value of γ is chosen to be 10 throughout this study. A larger value could not be chosen since numerical accuracy (with double precision numbers) of the matrix operations needed to compute $\tilde{\mathcal{P}}_{am}(t)$ rapidly decreased with increasing γ . At $\gamma = 10$, $\tilde{\mathcal{P}}_{am}(t)$ could be calculated with a relative accuracy of $\sim 10^{-4}$. In a system with $N_f = 9$, it has been observed that propagation of this error leads to $\mathcal{P}_{am}(\omega)$ having a relative accuracy of $\sim 10^{-4}$ even when the limits of integration are $[-10T, 10T]$ ($T \approx 61.7 [e^2 n^{1.5}/\epsilon_0 m^*]^{-1/2}$ for this system). (Errors are computed relative to a quadruple precision calculation.) As this range of integration was the largest in this study, we assume that this numerical error is negligible in all cases.

We can now discretize Eq. D4. To do this correctly with a minimal number of $\mathcal{P}_{am}(t)$ evaluations *i.e.* with the discretization time being the largest possible, the peak of interest must be at the origin. Hence, the quantity calculated is $\mathcal{P}_s(\omega) = \mathcal{P}_{am}(\omega + \omega_p)$, where ω_p the is expected peak position in $\mathcal{P}_{am}(\omega)$. In a first approximation this is roughly $\omega_0 = (E_i^g - E_f^g)/\hbar$ (< 0) where $E_{i,f}^g$ is the ground state energy of $\mathcal{H}_{i,f}^h$. It is found that ω_p is actually lower than this because the peak is dominated by the overlap of the ground state of \mathcal{H}_i^h with *excited* states of \mathcal{H}_f^h . ω_p is therefore calculated assuming that it is equal to the expectation value of ω in the distribution $\mathcal{P}_{am}(\omega)$:

$$\text{with } \omega_p = \omega_0 + \bar{\omega},$$

$$\text{where } \omega_0 = \frac{\epsilon_i^m - \epsilon_f^m}{\hbar} + \frac{\text{Tr}(\mathbf{\Omega}_i - \mathbf{\Omega}_f)}{2},$$

$$\text{and } \bar{\omega} = \frac{1}{i} \frac{d}{dt} e^{-i\omega_0 t} \tilde{\mathcal{P}}_{am}(t) \Big|_{t=0},$$

$$\mathcal{P}_s(\omega) = \frac{1}{2\pi} \int_{-T}^{+T} dt e^{-i(\omega + \omega_p)t} \tilde{\mathcal{P}}_{am}(t), \quad (\text{D5})$$

$$\omega = \frac{n\pi}{T}.$$

The above integration can be transformed into a summation without introducing any error if $\mathcal{P}_s(\omega)$ is zero for $|\omega| \geq \omega_M$. Since it is observed that $\mathcal{P}_s(\omega)$ is roughly Gaussian in shape, we assume that this is indeed the case with $\omega_M = 5 \times (3\sigma_\omega)$ where σ_ω^2 is the variance of ω in the distribution $\mathcal{P}_s(\omega)$ which is given by:

$$\sigma_\omega^2 = -\frac{d^2}{dt^2} e^{-i\omega_0 t} \tilde{\mathcal{P}}_{am}(t) \Big|_{t=0} - \bar{\omega}^2.$$

Eq. D4 is therefore discretized at a rate $\geq 2 \times \omega_M/2\pi$:²⁴

$$\text{with } \delta t = \frac{L}{T}, \quad L = \text{Int.} \left(\frac{T\omega_M}{\pi} \right),$$

$$\mathcal{P}_s(\omega) = \delta t \sum_{n=-L}^{L-1} e^{-i(\omega + \omega_p)t} \tilde{\mathcal{P}}_{am}(t), \quad (D6)$$

$$\omega = \frac{n\pi}{T}, \quad -L \leq n \leq L-1.$$

ω now takes on a finite number of values due to the discretization of the time domain. We make use of the symmetry $\tilde{\mathcal{P}}_{am}(-t) = [\tilde{\mathcal{P}}_{am}(t)]^*$ and avoid computing $\tilde{\mathcal{P}}_{am}(-t)$ for negative values of t . It must be noted that the large value of ω_M in relation to σ_ω is *not* forced due to integration errors (σ_ω is itself an overestimate of the variance due to the peak of interest since there are contributions from the other exponentially suppressed peaks) but due to the presence of a multivalued function (square root) in $\tilde{\mathcal{P}}_{am}(t)$ whose correct value has been inferred only by assuming that its phase does not vary abruptly between neighboring t values. It must also be noted that the derivatives needed to calculate $\bar{\omega}$ and σ_ω^2 are computed numerically. Finally, $\mathcal{P}_{am}(\omega)$ is calculated using:

$$\mathcal{P}_{am}(\omega) = \mathcal{P}_s(\omega - [\omega_p]), \quad (D7)$$

where $[\omega_p] = \omega_p$ in cases where there is no averaging over different $\mathcal{P}_s(\omega)$. However, in cases that demand such an average, $[\omega_p]$ is ω_p approximated to the nearest integral multiple of $\frac{\pi}{T}$ with σ_{est}^u being chosen conservatively so that T is the same for all the cases being averaged over. This error is expected to be negligible since it is verified that $\frac{\pi}{T} \ll 3\sigma_\omega$ for each of the spectra ($\mathcal{P}_{am}(\omega)$) in the average.

It must be noted that the computational scheme guarantees that $\mathcal{P}_{am}(\omega) \in \text{real numbers}$ since $\tilde{\mathcal{P}}_{am}(-t)$ has not been computed independently but has been equated to $[\tilde{\mathcal{P}}_{am}(t)]^*$. However it must be that $\mathcal{P}_{am}(\omega) \geq 0$. This condition serves as a good test for the validity of the approximations. It has been verified that for all our results the largest negative value is always a small fraction ($\sim 10^{-4}$) of the peak value of $\mathcal{P}_{am}(\omega)$.

Convergence criteria: In all the cases studied here the only functions needed to compute the potential energy terms (and their derivatives) are the gamma functions $\Gamma(a, b)$ (see Appendix A). As they have been numerically

evaluated with relative error $\lesssim 10^{-14}$ we extend the summations required to compute the potential (\tilde{V} in Eq. 1 as computed using Eq. A7) to achieve the same accuracy. Therefore the convergence criterion to determine the (classical) equilibrium configuration *i.e.* the upper bound on the root mean squared value of the force per electron at the end of the propagation with \mathcal{H}_i is chosen to be 10^{-14} natural force units ($= e^2 n / \epsilon_0$). Since the parameter λ_f in \mathcal{H}_f is chosen to be 10^3 times the natural scale of the same dimension, the convergence criterion with \mathcal{H}_f is weakened, the corresponding bound being 10^{-11} natural force units.

APPENDIX E: TRACE COMPUTATIONS WITH HARMONIC HAMILTONIANS

In this section we discuss how the trace operations appearing in Eq. D2 are evaluated:

$$Z = \left[e^{-\beta \mathcal{H}_i^h} \right],$$

$$G(t) = \text{Tr} \left[e^{-i\hbar^{-1} \mathcal{H}_f^h t} e^{i\hbar^{-1} \mathcal{H}_i^h (t + i\hbar\beta)} \right],$$

with \mathcal{H}_i^h given by Eq. 7, \mathcal{H}_f^h given by Eq. D3, and the operators in \mathcal{H}_f^h being related to those in \mathcal{H}_i^h through Eqs. 8, 9 and 10. We mention that the exact evaluation of the traces, which we do by adapting theoretical techniques developed in Ref. 27 in the context of coherent state properties, is a central feature of our calculations.

Z is the usual partition function for non-interacting bosons. It may be evaluated in the basis of eigenstates of \mathcal{H}_i^h to be:

$$Z = Z_0 \prod_{j=1}^{N_f} \left(1 - e^{-\beta \hbar \omega_{i,j}} \right), \quad Z_0 = e^{-\beta E_i^g},$$

$$\text{with } E_i^g = \hbar \frac{\text{Tr}[\mathbf{\Omega}_i]}{2} + \epsilon_i^m,$$

where $\omega_{i,j}$ is the diagonal element (phonon frequency) of the matrix $\mathbf{\Omega}_i$ appearing \mathcal{H}_i^h .

Theoretical results of Dodonov and Manko²⁷, that use the coherent state basis defined by the operators in \mathcal{H}_i^h , are employed in evaluating G . This basis, $|\zeta\rangle$, is defined by:

$$|\zeta\rangle = e^{\tilde{\mathbf{a}}_i^\dagger \zeta} |\mathbf{0}_i\rangle, \quad \mathbf{a}_{i,j} |\mathbf{0}_i\rangle = 0; \quad j = 1 \text{ to } N_f, \quad \langle \mathbf{0}_i | \mathbf{0}_i \rangle = 1.$$

where $|\mathbf{0}_i\rangle$ can be identified to be the normalized vacuum (ground) state of \mathcal{H}_i^h . ζ is a column vector of complex numbers of size N_f , and $\tilde{\mathbf{a}}_i^\dagger$ is a row vector of the $\mathbf{a}_{i,j}^\dagger$ operators. It can be shown that the states $|\zeta\rangle$ are overcomplete and that the trace of an arbitrary operator $\hat{\mathbf{O}}$ can be written as:

$$Tr \left[\hat{\mathbf{O}} \right] = \int \frac{d^{N_f} \zeta}{\pi^{N_f}} e^{-\zeta^\dagger \zeta} \langle \zeta | \hat{\mathbf{O}} | \zeta \rangle .$$

G may therefore be evaluated, using additionally the cyclic permutation invariance of the trace operation and knowing the action of the exponential of the number operators ($\mathbf{a}_{i,j}^\dagger \mathbf{a}_{i,j}$) on the coherent states, as:

$$G(t) = Z_0 e^{it\hbar^{-1} E_i^g} \int \frac{d^{N_f} \zeta}{\pi^{N_f}} e^{-\zeta^\dagger \zeta} \langle \mu | \mathcal{U} | \nu \rangle , \quad (E1)$$

$$\mathcal{U} = e^{-i\hbar^{-1} \hat{\mathcal{H}}_f^h t} , \quad \mu = \mathbf{E}^* \zeta , \quad \nu = \mathbf{E} \zeta ,$$

with $\mathbf{E} = e^{(-it - \beta\hbar) [\Omega_i]/2}$.

Therefore, matrix elements of the “propagator” \mathcal{U} corresponding to $\hat{\mathcal{H}}_f^h$ in the basis $|\zeta\rangle$ must be evaluated. It must be noted that this point of view is consistent only if the time variable t that appears *within* $\hat{\mathcal{H}}_f^h$ (Eq. D3) is treated as a constant parameter. This parameter is therefore held fixed at $t_0 \neq 0$ and then the matrix element is evaluated for all t . Of interest would be the value when $t = t_0$. (It is assumed that the $t_0 = 0$ value is equal to the limiting value as $t_0 \rightarrow 0$.) In other words, $\hat{\mathcal{H}}_f^h$ is viewed as a time independent Hamiltonian. Further, using Eqs. 8, 9 and 10 it can be seen that $\hat{\mathcal{H}}_f^h$ is a second order polynomial in the operators $\mathbf{a}_{i,j}$ and $\mathbf{a}_{i,j}^\dagger$. The required matrix elements for the most generic time dependent Hamiltonian that is of the same form has been computed by Dodonov and Manko²⁷ in a totally different context - we briefly review their solution and then specialize to our case.

The matrix elements of the propagator corresponding to the following Hamiltonian are evaluated in the coherent state basis:

$$\frac{\mathcal{H}}{\hbar} = [\tilde{\mathbf{a}} \tilde{\mathbf{a}}^\dagger] \left\{ \frac{\mathbf{K}}{2} \left[\begin{array}{c} \mathbf{a} \\ \mathbf{a}^\dagger \end{array} \right] + [\mathbf{s}] \right\} + \mathbf{r} , \quad (\mathbf{K}^T = \mathbf{K})$$

where the matrix $[\mathbf{K}]$, the vector $[\mathbf{s}]$ and the number \mathbf{r} are arbitrary complex functions of time (t). (The subscript i under the operators has been dropped.) The corresponding propagator \mathcal{U} (and its inverse \mathcal{U}^{-1}) may be defined through its equation of motion together with an initial condition:

$$i\hbar \frac{d\mathcal{U}}{dt} = \mathcal{H}\mathcal{U} , \quad \mathcal{U}(t=0) = \mathcal{I} \quad (E2)$$

$$i\hbar \frac{d\mathcal{U}^{-1}}{dt} = -\mathcal{U}^{-1}\mathcal{H} , \quad \mathcal{U}^{-1}(t=0) = \mathcal{I}$$

It can be shown that an invertible operator can be defined, up to a multiplicative constant, by its action on *all* the canonically conjugate operators, *i.e.* if two invertible operators \mathcal{U}_x and \mathcal{U}_y satisfy

$$\left[\begin{array}{c} \mathbf{b} \\ \bar{\mathbf{b}} \end{array} \right] = \mathcal{U}_{x,(y)} \left[\begin{array}{c} \mathbf{a} \\ \tilde{\mathbf{a}} \end{array} \right] \mathcal{U}_{x,(y)}^{-1} \quad (E3)$$

then it must be that $\mathcal{U}_x = c\mathcal{U}_y$, where c is a (non zero) c-number. This is now used to evaluate the propagator \mathcal{U} (or equivalently its matrix elements). The multiplicative freedom in \mathcal{U} is finally lifted using its equation of motion together with the initial condition (Eq. E1). Note that the elements of $\bar{\mathbf{b}}$ need not be the Hermitian conjugates of those in \mathbf{b} as the operator \mathcal{U} need not be unitary (for it could correspond to a non-Hermitian Hamiltonian).

The above procedure to determine \mathcal{U} can be implemented only if the operators \mathbf{b} and $\bar{\mathbf{b}}$ are known. They can be determined from their equation of motion together with the initial condition which are obtained using Eqs. E2 and E3:

$$i\hbar \frac{d}{dt} \left[\begin{array}{c} \mathbf{b} \\ \bar{\mathbf{b}} \end{array} \right] = \left\{ \mathcal{H} , \left[\begin{array}{c} \mathbf{b} \\ \bar{\mathbf{b}} \end{array} \right] \right\} , \quad \left[\begin{array}{c} \mathbf{b} \\ \bar{\mathbf{b}} \end{array} \right] (t=0) = \left[\begin{array}{c} \mathbf{a} \\ \mathbf{a}^\dagger \end{array} \right] \quad (E4)$$

where the curly brackets now represent the commutator. The above equations are solved by making the following *anzatz* which is motivated by \mathcal{H} being a second order polynomial in the operators \mathbf{a}_j and \mathbf{a}_j^\dagger :

$$\left[\begin{array}{c} \mathbf{b} \\ \bar{\mathbf{b}} \end{array} \right] = [\Lambda] \left[\begin{array}{c} \mathbf{a} \\ \mathbf{a}^\dagger \end{array} \right] + [\lambda] , \quad (E5)$$

where Λ (λ) is a c-number matrix (vector) function of t . Substituting the above into Eq. E4 it can be seen that the anzatz is successful as it leads to the following differential equations with appropriate initial conditions (the linear independence of the operators \mathbf{a}_j , \mathbf{a}_j^\dagger and \mathcal{I} has been used):

$$i \frac{d\Lambda}{dt} = -\Lambda \Sigma \mathbf{K} , \quad \Lambda(t=0) = \mathbf{I} , \quad \Sigma = \left[\begin{array}{cc} \mathbf{0} & \mathbf{I} \\ -\mathbf{I} & \mathbf{0} \end{array} \right] ,$$

$$i \frac{d\lambda}{dt} = -\Lambda \Sigma \mathbf{s} , \quad \lambda(t=0) = \mathbf{0} . \quad (E6)$$

The above may be solved for Λ and λ . An important property of the solution is that the matrix Λ is canonical for all t :

$$\Lambda^T \Sigma \Lambda = \Sigma . \quad (E7)$$

Eq. E3 may now be used to evaluate the matrix elements of \mathcal{U} in the basis $|\zeta\rangle$ after substituting for the operators $[\mathbf{b}]$ and $[\bar{\mathbf{b}}]$ using Eq. E5 with Λ and λ being the solutions of Eq. E6. The matrix elements of Eq. E3 (after multiplying from the right by \mathcal{U}) in this basis reads, with

$$\Lambda = \left[\begin{array}{cc} \Lambda_1 & \Lambda_2 \\ \Lambda_3 & \Lambda_4 \end{array} \right] , \quad \lambda = \left[\begin{array}{c} \lambda_1 \\ \lambda_2 \end{array} \right] , \quad \langle \mu | \mathcal{U}(t) | \nu \rangle = U(\mu^*, \nu, t) ,$$

$$\left\{ \Lambda_1 \frac{\partial}{\partial \mu^\dagger} + \Lambda_2 \mu^* + \lambda_1 \right\} U(\mu^*, \nu, t) = \nu U(\mu^*, \nu, t) ,$$

$$\left\{ \Lambda_3 \frac{\partial}{\partial \mu^\dagger} + \Lambda_4 \mu^* + \lambda_2 \right\} U(\mu^*, \nu, t) = \frac{\partial}{\partial \nu^T} U(\mu^*, \nu, t) .$$

The above can be solved (assuming the existence of Λ_1^{-1} and using Eq. E7) for the μ^* and ν dependence of $U(\mu^*, \nu, t)$. The unsolved time dependence appears as an arbitrary multiplicative integration constant:

$$\ln [U(\mu^*, \nu, t)] = \frac{1}{2} [-\mu^\dagger \Lambda_1^{-1} \Lambda_2 \mu^* + \nu^T \Lambda_3 \Lambda_1^{-1} \nu] + \mu^\dagger \Lambda_1^{-1} [\nu - \lambda_1] + \nu^T [\lambda_2 - \Lambda_3 \Lambda_1^{-1} \lambda_1] + f(t). \quad (\text{E8})$$

Using the above and evaluating the matrix elements of Eq. E2 (for \mathcal{U}), it may be seen (using Eqs. E6 and E7) that Eq. E2 is indeed satisfied in its μ^* and ν dependences, and it leads to the following equations determining f :

$$\begin{aligned} \frac{df}{dt} &= \frac{1}{2} \frac{d}{dt} \left[\lambda_1^T \Lambda_3 \Lambda_1^{-1} \lambda_1 \right], \\ - \left[i\mathbf{r} + \frac{1}{2} \text{Tr} \left[\Lambda_1^{-1} \frac{d\Lambda_1}{dt} \right] + \frac{d\lambda_2^T}{dt} \lambda_1 \right] &, \quad f(t=0) = 0. \end{aligned} \quad (\text{E9})$$

Hence, as argued previously, Eq. E3 leaves only a c-number multiplicative freedom in \mathcal{U} which is lifted by using Eq. E2. This completes the generic solution of the matrix elements of interest.

We now specialize to our case to evaluate G (Eq. E4) by identifying \mathcal{H} to be $\hat{\mathcal{H}}_f^h$. This implies (using Eqs. 8, 9, 10 and D3):

$$\mathbf{K} = \mathbf{T}^T \dot{\mathbf{\Omega}}_f \mathbf{T}, \quad \mathbf{s} = \mathbf{T}^T \dot{\mathbf{\Omega}}_f \mathbf{w}, \quad \mathbf{r} = \frac{\mathbf{w}^T \dot{\mathbf{\Omega}}_f \mathbf{w}}{2} + \hbar^{-1} \epsilon_f^m.$$

The above may now be used to obtain explicit solutions to Eqs. E6 and E9 - as mentioned previously the time t that appears within $\dot{\mathbf{\Omega}}_f$ is treated as a constant and then the solution is evaluated for t being equal to this constant. This gives, with

$$\mathbf{P} = e^{[i\Omega_f t + \mathbf{D}_\gamma]}, \quad \dot{\mathbf{P}} = e^{[-i\Omega_f t - \mathbf{D}_\gamma]},$$

and knowing (using Eqs. 9 and B4) that \mathbf{T} is canonical, i.e. $\mathbf{T}^T \mathbf{\Sigma} \mathbf{T} = \mathbf{\Sigma}$:

$$\begin{aligned} \Lambda_1(t) &= \mathbf{U}^\dagger \mathbf{P} \mathbf{U} - \mathbf{V}^T \dot{\mathbf{P}} \mathbf{V}^*, \\ \Lambda_2(t) &= \mathbf{U}^\dagger \mathbf{P} \mathbf{V} - \mathbf{V}^T \dot{\mathbf{P}} \mathbf{U}^*, \\ \Lambda_3(t) &= \mathbf{U}^T \dot{\mathbf{P}} \mathbf{V}^* - \mathbf{V}^\dagger \mathbf{P} \mathbf{U}, \\ \Lambda_4(t) &= \mathbf{U}^T \dot{\mathbf{P}} \mathbf{U}^* - \mathbf{V}^\dagger \mathbf{P} \mathbf{V}, \\ \lambda_1(t) &= \mathbf{U}^\dagger [\mathbf{P} - \mathbf{I}] \Delta - \mathbf{V}^T [\dot{\mathbf{P}} - \mathbf{I}] \Delta^*, \\ \lambda_2(t) &= \mathbf{U}^T [\dot{\mathbf{P}} - \mathbf{I}] \Delta^* - \mathbf{V}^\dagger [\mathbf{P} - \mathbf{I}] \Delta, \\ f(t) &= \frac{1}{2} \left[\lambda_1^T \Lambda_3 \Lambda_1^{-1} \lambda_1 - \ln (\det \Lambda_1) \right] \\ &+ \frac{1}{4} \left[\lambda_1^\dagger \lambda_1 - \lambda_2^\dagger \lambda_2 - 2 \lambda_2^\dagger \lambda_1^* \right] \\ &- \Delta^\dagger \text{Sinh} [\mathbf{D}_\gamma] \{2 \text{Cos} [\Omega_f t] - \text{Cosh} [\mathbf{D}_\gamma]\} \Delta \\ &- i \Delta^\dagger \text{Cosh} [\mathbf{D}_\gamma] \text{Sin} [\Omega_f t] \Delta - i \hbar^{-1} \epsilon_f^m t. \end{aligned} \quad (\text{E10})$$

$G(t)$ (Eq. E1) is now determined as the matrix element $\langle \mu | \mathcal{U} | \nu \rangle = U(\mu^*, \nu, t)$ (using Eq. E10) is given by Eq. E8. (Dodonov and Manko²⁷ also obtain this matrix element for the special case of $\mathbf{\Omega}_f \propto \mathbf{I}$ and $\mathbf{D}_\gamma = \mathbf{0}$) Further, the integral in Eq. E1 may be carried out analytically (assuming the positive definiteness of the appropriate matrix) to give:

$$\begin{aligned} \ln \left[\frac{G(t)}{Z_0} \right] &= i \hbar^{-1} E_i^g + f(t) \\ &+ \frac{\ln \{\det [\mathbf{A} \mathbf{\Sigma}_+]\}}{2} + \frac{1}{2} \mathbf{F}^T \mathbf{A}^{-1} \mathbf{F}, \\ \text{where } \mathbf{\Sigma}_+ &= \begin{bmatrix} \mathbf{0} & \mathbf{I} \\ \mathbf{I} & \mathbf{0} \end{bmatrix}, \quad \mathbf{A} = \mathbf{\Sigma}_+ - \dot{\mathbf{E}} \mathbf{J} \dot{\mathbf{E}}, \quad \mathbf{F} = \dot{\mathbf{E}} \mathbf{l}, \\ \text{with } \mathbf{J} &= \begin{bmatrix} \Lambda_1^{-1} \Lambda_2 & \Lambda_1^{-1} \\ [\Lambda_1^{-1}]^T & \Lambda_3 \Lambda_1^{-1} \end{bmatrix}, \quad \dot{\mathbf{E}} = \begin{bmatrix} \mathbf{E} & \mathbf{0} \\ \mathbf{0} & \mathbf{E} \end{bmatrix}, \\ \text{and } \mathbf{l} &= \begin{bmatrix} -\lambda_1 \\ \lambda_2 - \Lambda_3 \Lambda_1^{-1} \lambda_1 \end{bmatrix}. \end{aligned} \quad (\text{E11})$$

This completes the analytical determination of the required trace operations.

¹ E.P. Wigner, Phys. Rev. **46**, 1002 (1934). For a current status of the subject see, for example, the review articles by H.A. Fertig (p.51) and M. Shayegan (p.343) in *Perspectives in Quantum Hall Effects*, edited by S. Das Sarma and A. Pinczuk (Wiley, New York, 1997).

² C.C. Grimes and G. Adams, Phys. Rev. Lett. **42**, 795 (1979).

³ B. Tanatar and D.M. Ceperley, Phys. Rev. B **39**, 5005 (1989).

⁴ K. von Klitzing, G. Dorda and M. Pepper, Phys. Rev. Lett. **45**, 494 (1980).

⁵ D.C. Tsui, H.L. Stormer and A.C. Gossard, Phys. Rev. Lett. **48**, 1559 (1982).

⁶ R. Price, *The Two-Dimensional Wigner Solid* (PhD thesis, University of California at San Diego, 1993).

⁷ I.V. Kukushkin, V.I. Falko, R.J. Haug, K. von Klitzing, K. Eberl and K. Totemayer, Phys. Rev. Lett. **72**, 3594 (1994).

⁸ I.V. Kukushkin, N.J. Pulford, K. von Klitzing, R. Haug and K. Ploog, Physica B **184**, 38 (1993).

⁹ I.V. Kukushkin, K. von Klitzing, K. Ploog and V.B. Timofeev, Phys. Rev. B **40**, 7788 (1989).

¹⁰ H. Buhmann, W. Joss, K.v. Klitzing, I.V. Kukushkin, A.S. Plaut, G. Martinez, K. Ploog and V.B. Timofeev, Phys. Rev. Lett. **66**, 926 (1991).

¹¹ P. Johansson and J.M. Kinaret, Phys. Rev. Lett. **71**, 1435 (1993).

¹² G.D. Mahan, *Many-Particle Physics* (Plenum, New York, 1993).

¹³ J.P. Eisenstein, L.N. Pfeiffer and K.W. West, Phys. Rev. Lett. **69**, 3804 (1992).

- ¹⁴ H.A. Fertig, D.Z. Liu and S. Das Sarma, Phys. Rev. Lett. **70**, 1545 (1993); D.Z. Liu, H.A. Fertig and S. Das Sarma, Phys. Rev. B **54**, 13915 (1996) and references therein.
- ¹⁵ L. Bonsall and A.A. Maradudin, Phys. Rev. B **15**, 1959 (1977).
- ¹⁶ B.R.A. Nijboer and F.W. Dewette, Physica **23**, 309 (1957).
- ¹⁷ Y.M. Vilk and Y.P. Monarkha, Sov. J. Low. Temp. Phys. **10**, 469 (1984).
- ¹⁸ V.A. Schweigert and F.M. Peeters, Phys. Rev. B **51**, 7700 (1995).
- ¹⁹ K. Maki and X. Zotos, Phys. Rev. B. **28**, 4349 (1983).
- ²⁰ F.C. Zhang and S. Das Sarma, Phys. Rev. B **33**, 2903 (1986).
- ²¹ I.M. Ruzin, S.Marianer and B.I. Shklovskii, Phys. Rev. B **46**, 3999 (1992).
- ²² T. Kawamura and S. Das Sarma, Solid State Commun. **100**, 411 (1996).
- ²³ C. Lanczos, J.SIAM Numer. Anal. Ser. B **1**, 86 (1964).
- ²⁴ W.H. Press, S.A. Teukolsky, W.T. Vetterling, B.P. Flannery, *Numerical Recipes*, (Cambridge University Press, New York, 1992).
- ²⁵ S.K. Yip, Phys. Rev. B **43**, 1707 (1991).
- ²⁶ C. Cohen-Tannoudji, J. Dupont-Roc and G. Grynberg, *Photons and Atoms* (Wiley, New York, 1989).
- ²⁷ V.V. Dodonov and V.I. Manko, Proc. Lebedev Phys. Inst., **183**, 263 (1987).